NUCLEAR DATA AND MEASUREMENTS SERIES

ANL/NDM-124

THE THICK-TARGET $^{9}Be(d,n)$ NEUTRON SPECTRA FOR DEUTERON ENERGIES BETWEEN 2.6 AND 7.0-MeV

NOVEMBER 1991

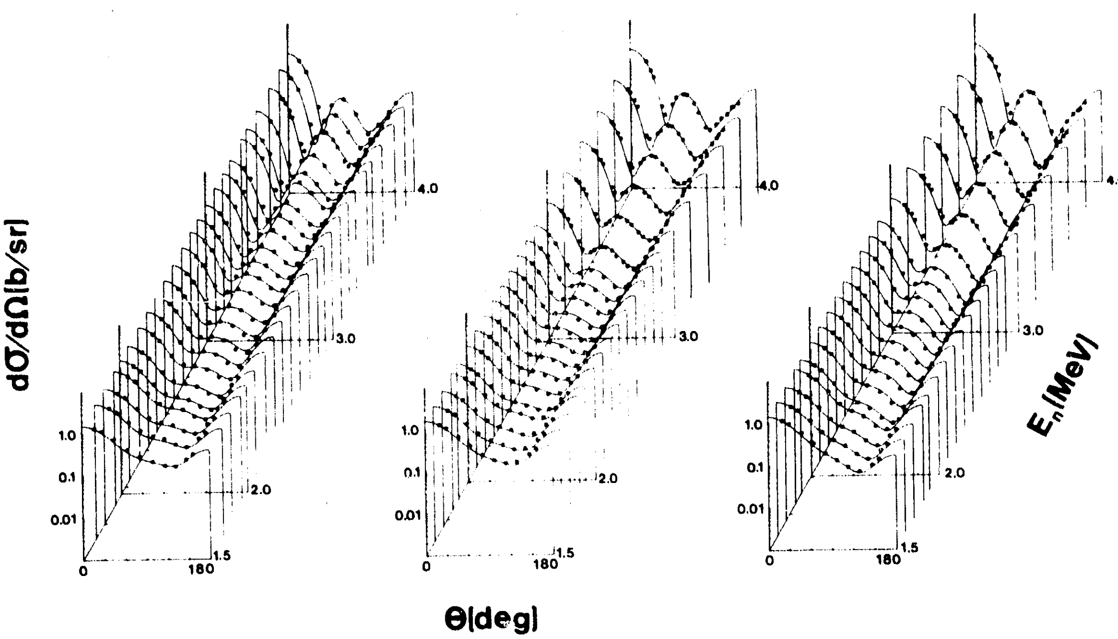

ARGONNE NATIONAL LABORATORY, ARGONNE, ILLINOIS

Operated by THE UNIVERSITY OF CHICAGO
for the U. S. DEPARTMENT OF ENERGY
under Contract W-31-109-Eng-38

Argonne National Laboratory, with facilities in the states of Illinois and Idaho, is owned by the United States government, and operated by The University of Chicago under the provisions of a contract with the Department of Energy.

Reproduced from the best available copy.

Available to DOE and DOE contractors from the
Office of Scientific and Technical Information
P.O. Box 62
Oak Ridge, TN 37831
Prices available from (615) 576-8401, FTS 626-8401

Available to the public from the
National Technical Information Service
U.S. Department of Commerce
5285 Port Royal Road
Springfield, VA 22161

ANL/NDM--124

DE92 007618

ANL/NDM-124

THE THICK-TARGET ^{9}Be(d,n) NEUTRON SPECTRA FOR DEUTERON ENERGIES BETWEEN 2.6 AND 7.0-MeV*

by

J. W. Meadows

November 1991

Engineering Physics Division
ARGONNE NATIONAL LABORATORY
9700 South Cass Avenue
Argonne, Illinois 60439
U.S.A.

*This work was supported by the U. S. Department of Energy, Energy Research Programs, under Contract W-31-109-Eng-38.

NUCLEAR DATA AND MEASUREMENTS SERIES

The Nuclear Data and Measurements Series presents results of studies in the field of microscopic nuclear data. The primary objective is the dissemination of information in the comprehensive form required for nuclear technology applications. This Series is devoted to: a) measured microscopic nuclear parameters, b) experimental techniques and facilities employed in measurements, c) the analysis, correlation and interpretation of nuclear data, and d) the evaluation of nuclear data. Contributions to this Series are reviewed to assure technical competence and, unless otherwise stated, the contents can be formally referenced. This Series does not supplant formal journal publication, but it does provide the more extensive information required for technological applications (e.g., tabulated numerical data) in a timely manner.

TABLE OF CONTENTS

INFORMATION ABOUT OTHER ISSUES OF THE ANL/NDM SERIES

A list of titles and authors for all the previous issues appears in reports of the series. The list for reports ANL/NDM-1 through ANL/NDM-75 appears in ANL/NDM-76, and ANL/NDM-91 contains the list for reports ANL/NDM-76 through ANL/NDM-90. Below is the list for ANL/NDM-91 up to the current report. Requests for a complete list of titles, or for copies of previous reports, should be directed to:

Section Secretary
Applied Nuclear Physics Section
Engineering Physics Division
Building 316
Argonne National Laboratory
9700 South Cass Avenue
Argonne, Illinois 60439
U.S.A.

ANL/NDM-91 A.B. Smith, P.T. Guenther and R.D. Lawson, *On the Energy Dependence of the Optical Model of Neutron Scattering from Niobium*, May 1985.

ANL/NDM-92 Donald L. Smith, *Nuclear Data Uncertainties (Vol.-I): Basic Concepts of Probability*, December 1988.

ANL/NDM-93 D.L. Smith, J.W. Meadows and M.M. Bretscher, *Integral Cross-section Measurements for* $^{7}Li(n,n't)^{4}He$, $^{27}Al(n,p)^{27}Mg$, $^{27}Al(n,a)^{24}Na$, $^{58}Ni(n,p)^{58}Co$, *and* $^{60}Ni(n,p)^{60}Co$ *Relative to* ^{238}U *Neutron Fission in the Thick-target* $^{9}Be(d,n)^{10}B$ *Spectrum at* $E_d = 7$ *MeV*, October 1985.

ANL/NDM-94 A.B. Smith, D.L. Smith, P. Rousset, R.D. Lawson and R.J. Howerton, *Evaluated Neutronic Data File for Yttrium*, January 1986.

ANL/NDM-95 Donald L. Smith and James W. Meadows, *A Facility for High-intensity Neutron Irradiations Using Thick-target Sources at the Argonne Fast-neutron Generator*, May 1986.

ANL/NDM-96 M. Sugimoto, A.B. Smith and P.T. Guenther, *Ratio of the Prompt-fission-neutron Spectrum of Plutonium-239 to that of Uranium-235*, September 1986.

ANL/NDM-97 J.W. Meadows, *The Fission Cross Sections of* ^{230}Th, ^{232}Th, ^{233}U, ^{234}U, ^{236}U, ^{238}U, ^{237}Np, ^{239}Pu, *and* ^{242}Pu *Relative* ^{235}U *at 14.74 MeV Neutron Energy*, December 1986.

ANL/NDM-98 J.W. Meadows, *The Fission Cross Section Ratios and Error Analysis for Ten Thorium, Uranium, Neptunium and Plutonium Isotopes at 14.74-MeV Neutron Energy*, March 1987.

ANL/NDM-99 Donald L. Smith, *Some Comments on the Effects of Long-range Correlations in Covariance Matrices for Nuclear Data*, March 1987.

ANL/NDM-100 A.B. Smith, P.T. Guenther and R.D. Lawson, *The Energy Dependence of the Optical-model Potential for Fast-neutron Scattering from Bismuth*, May 1987.

ANL/NDM-101 A.B. Smith, P.T. Guenther, J.F. Whalen and R.D. Lawson, *Cobalt: Fast Neutrons and Physical Models*, July 1987.

ANL/NDM-102 D. L Smith, *Investigation of the Influence of the Neutron Spectrum in Determinations of Integral Neutron Cross-Section Ratios*, November 1987.

ANL/NDM-103 A.B. Smith, P.T. Guenther and B. Micklich, *Spectrum of Neutrons Emitted From a Thick Beryllium Target Bombarded With 7 MeV Deuterons*, January 1988.

ANL/NDM-104 L.P. Geraldo and D.L. Smith, *Some Thoughts on Positive Definiteness in the Consideration of Nuclear Data Covariance Matrices*, January 1988.

ANL/NDM-105 A.B. Smith, D.L. Smith, P.T. Guenther, J.W. Meadows, R.D. Lawson, R.J. Howerton, and T. Djemil, *Neutronic Evaluated Nuclear-Data File for Vanadium*, May 1988.

ANL/NDM-106 A.B. Smith, P.T. Guenther, and R.D. Lawson, *Fast-Neutron Elastic Scattering from Elemental Vanadium*, March 198[illegible]

ANL/NDM-107 P. Guenther, R. Lawson, J. Meadows, M. Sugimoto, A. Smith, D. Smith, and R. Howerton, *An Evaluated Neutronic Data File for Elemental Cobalt*, August 1988.

ANL/NDM-108 M. Sugimoto, P.T. Guenther, J.E. Lynn, A.B. Smith, and J.F. Whalen, *Some Comments on the Interaction of Fast-Neutrons with Beryllium*, November 1988.

ANL/NDM-109 P.T. Guenther, R.D. Lawson, J.W. Meadows, A.B. Smith, D.L. Smith, and M. Sugimoto, *An Evaluated Neutronic Data File for Bismuth*, November 1989.

ANL/NDM-110 D.L. Smith and L.P. Geraldo, *A Vector Model for Error Propagation*, March 1989.

ANL/NDM-111 J.E. Lynn, *Fifty Years of Nuclear Fission*, June 1989.

ANL/NDM-112 S. Chiba, P.T. Guenther, and A.B. Smith, *Some Remarks on the Neutron Elastic- and Inelastic-Scattering Cross Sections of Palladium*, May 1989.

ANL/NDM-113 J.E. Lynn, *Resonance Effects in Neutron Scattering Lengths*, June 1989.

ANL/NDM-114 A.B. Smith, R.D. Lawson, and P.T. Guenther, *Ambiguities in the Elastic Scattering of 8 MeV Neutrons from Adjacent Nuclei*, October 1989.

ANL/NDM-115 A.B. Smith, S. Chiba, D.L. Smith, J.W. Meadows, P.T. Guenther, R.D. Lawson, and R.J. Howerton, *Evaluated Neutronic File for Indium*, January 1990.

ANL/NDM-116 S. Chiba, P.T. Guenther, R.D. Lawson, and A.B. Smith, *Neutron Scattering from Elemental Indium, the Optical Model, and the Bound-State Potential*, June 1990.

ANL/NDM-117 Donald L. Smith and Luiz P. Geraldo, *An Evaluation of the Nb-93(n,n')Nb-93m Dosimeter Reaction for ENDF/B-VI*, November 1990.

ANL/NDM-118 J. W. Meadows, *Characteristics of the Samples in the FNG Fission Deposit Collection*, December 1990.

ANL/NDM-119 S. Chiba, P. T. Guenther, A. B. Smith and R. D. Lawson, *Fast-Neutron Interaction with Elemental Zirconium and the Dispersive Optical Model,* April 1991.

ANL/NDM-120 A. B. Smith, P. T. Guenther, J. F. Whalen and S. Chiba, *Fast-Neutron Total and Scattering Cross Sections of Ni-58 and Nuclear Models*, July 1991.

ANL/NDM-121 Satoshi Chiba and Donald L. Smith, *A Suggested Procedure for Resolving an Anomaly in Least-Squares Data Analysis Known as "Peelle's Pertinent Puzzle" and General Implications for Nuclear Data Evaluation*, February 1990.

ANL/NDM-122 Dominique Feautrier and Donald L. Smith, *Development and Testing of aDeuterium Gas Target Assembly for Neutron Production Via the H-2(D<N)He-3 kReaaction at a Low-Energy Accelerator Facility*, August 1991.

ANL/NDM-123 Donald L. Smith and Edward T. Cheng, *A Review of Nuclear Data Needs and their Status for Fusion Reactor Technology with Some Suggestions on a Strategy to Satisfy the Requirements*, September 1991.

THE THICK-TARGET $^{9}Be(d,n)$ NEUTRON SPECTRA FOR DEUTERON ENERGIES BETWEEN 2.6 AND 7.0-MeV*

by

J. V. Meadows
November 1991

Engineering Physics Division
Argonne National Laboratory
Argonne, Illinois 60439

ABSTRACT

The measurement of the zero deg. neutron spectra and yields from deuterons incident on thick beryllium metal targets is described. ^{235}U and ^{238}U fission ion chambers were used as neutron detectors to span the neutron energy range above 0.05-MeV with a time resolution of $\leq$ 3 nanosec. Measurements were made for incident deuteron energies from 2.6 to 7.0-MeV, at 0.4-MeV intervals, using time-of-flight techniques with flight paths of 2.7 and 6.8 meters. The results are presented in graphical form and in tables.

---

*This work was supported by the U. S. Department of Energy, Energy Research Programs, under Contract W-31-109-Eng-38.

I. INTRODUCTION

The availability of high-intensity, broad-spectrum sources of fast neutrons is of increasing importance for uses as diverse as radiotherapy and materials-damage studies. If their spectral shapes are well determined, and if they can be pulsed, such sources are also useful for measuring the energy-dependent efficiency of many neutron detectors. Integral measurements in high-intensity neutron fields with well-characterized spectra provide a convenient method of quickly testing nuclear-reaction data, and can provide very useful information on the production of some long-lived isotopes that could not otherwise be obtained. Also, it has been shown that if measurements are made in several different spectra, then differential cross information can be obtained.[1]

Deuterons with energies of several MeV incident on a thick beryllium target are particularly favored for such intense sources. The target material is beryllium metal which can be machined into convenient shapes, is stable, and is capable of withstanding beam currents of 50-100 μamp with elementary target designs and cooling. The maximum Q-value of the principal reaction, $^{9}Be(d,n)^{10}B$, is fairly large and positive (+4.36-MeV). The reaction may proceed to a number of excited states in ^{10}B which tends to smooth and broaden the spectrum and enhance the total-neutron yield. In addition, there are several multi-body reaction channels such as (d,2n), (d,pn) and (d,p2n) with negative Q-values. If the deuteron energy is above their thresholds, these reactions may enhance the low-energy neutron yield. Low-energy neutrons are of particular interest in radiotherapy because of their increased-biological effectiveness.

For our purposes, the important use of such a source is the production and testing of neutron-reaction data. Furthermore, the dependence of the spectrum shape on the incident deuteron energy opens the possibility of tailoring (within limits) the spectra for specific problems. There have been several measurements of the neutron spectra from deuteron bombardment of both thin and thick beryllium targets as well as of some angular distributions (refs. 2-9). However, many of these measurements were made at deuteron energies well above our region of interest. Also, most of these measurements used hydrogenous scintillators as neutron detectors and did not cover that part of the neutron spectra below 1 - 2 MeV. Consequently, we have undertaken a systematic study of the Be(d,n) thick-target spectra and their angular distributions as a function of incident-deuteron energy. Measurements of the spectrum and angular distribution at 7-MeV have been reported earlier.[7] In this report, we give the results of measurements of the zero deg. neutron spectra for deuteron energies of 2.6- to 7.0-MeV in 0.4-MeV steps. They cover the full neutron-energy range above about 50-keV, but the emphasis is on the lower energies.

II. EXPERIMENTAL METHOD

The neutron spectra were measured by fairly conventional time-of-flight techniques using ^{235}U and ^{238}U fission ion chambers as neutron detectors. All spectrum measurements were made at zero deg. with flight paths of approximately 2.7 and 7 m. A phototube with a small plastic scintillator attached was placed about 1 meter downstream from the neutron detector. This measured the time spectrum of the target gamma rays which were used to monitor the quality of the pulsed beam. Most of the measurements were made with pulse repetition times of 500 and 1000 nanosec. A few measurements were made at 2000 nanosec. Spectra were recorded in 512 channels for all repetition times.

Although the time resolution of hydrogenous scintillators is less and the neutron detection efficiency is usually much greater, fission detectors do have some definite advantages: First, they are insensitive to gamma rays. Second, the ^{235}U detector has no low-energy limit for neutron detection. Third, the energy dependence of the fission detectors is determined primarily by the ^{235}U and ^{238}U fission cross sections. If better data is available in the future, the results can be easily corrected. However, these cross sections are believed to be rather well determined so any uncertainty from this error source is small. A corollary feature is the good stability of the detector efficiency and its low sensitivity to threshold levels. The low efficiency of the fission detectors is a definite problem, and time considerations limited flight paths to $\lesssim$ 7 meters. This limitation on the flight path combined with the poorer time resolution did limit the quality of the spectra obtained in this measurement to some extent.

III. APPARATUS

1. <u>Neutron</u> <u>Source:</u> Deuterons, accelerated by the Argonne Tandem Dynamitron Accelerator, strike a thick (~ 0.75 mm) beryllium metal target and produce neutrons by Be(d,xn) reactions. The incident deuteron energy, ranging from 2.6 to 7.0-MeV, is controlled by a 90-deg. analyzing magnet and slit feed-back system, calibrated by methods described in ref. 10. For an unbunched deuteron beam, energy control of ± 1 keV is readily achieved. However, the buncher imposes an energy spread of ~ 10 keV. Deuteron beam pulses 20 - 30 ns wide are bunched by a double klystron buncher to produce pulse widths of < 2 nanosec at the target. Pulse repetition times of 0.500 to 16.00 μsec (2 to 0.0625 MHz) are available.

   A measurement of the total-deuteron charge incident on the beryllium target accompanied all spectra. In order to reduce the leakage current, all the water cooling lines were disconnected and only air cooling was used. For these conditions, the leakage current correction was ~ 0.05 μamp.

   All the spectrum measurements were made at zero degrees, using the shielded neutron-irradiation cavity described in ref. 11 to contain the neutron source. The cavity is formed by a concrete block of various sizes stacked to produce walls > 1 m thick. The interior is lined with about 20 cm of polyethylene block, a 0.5 mm thick layer of cadmium sheet and, finally, with a

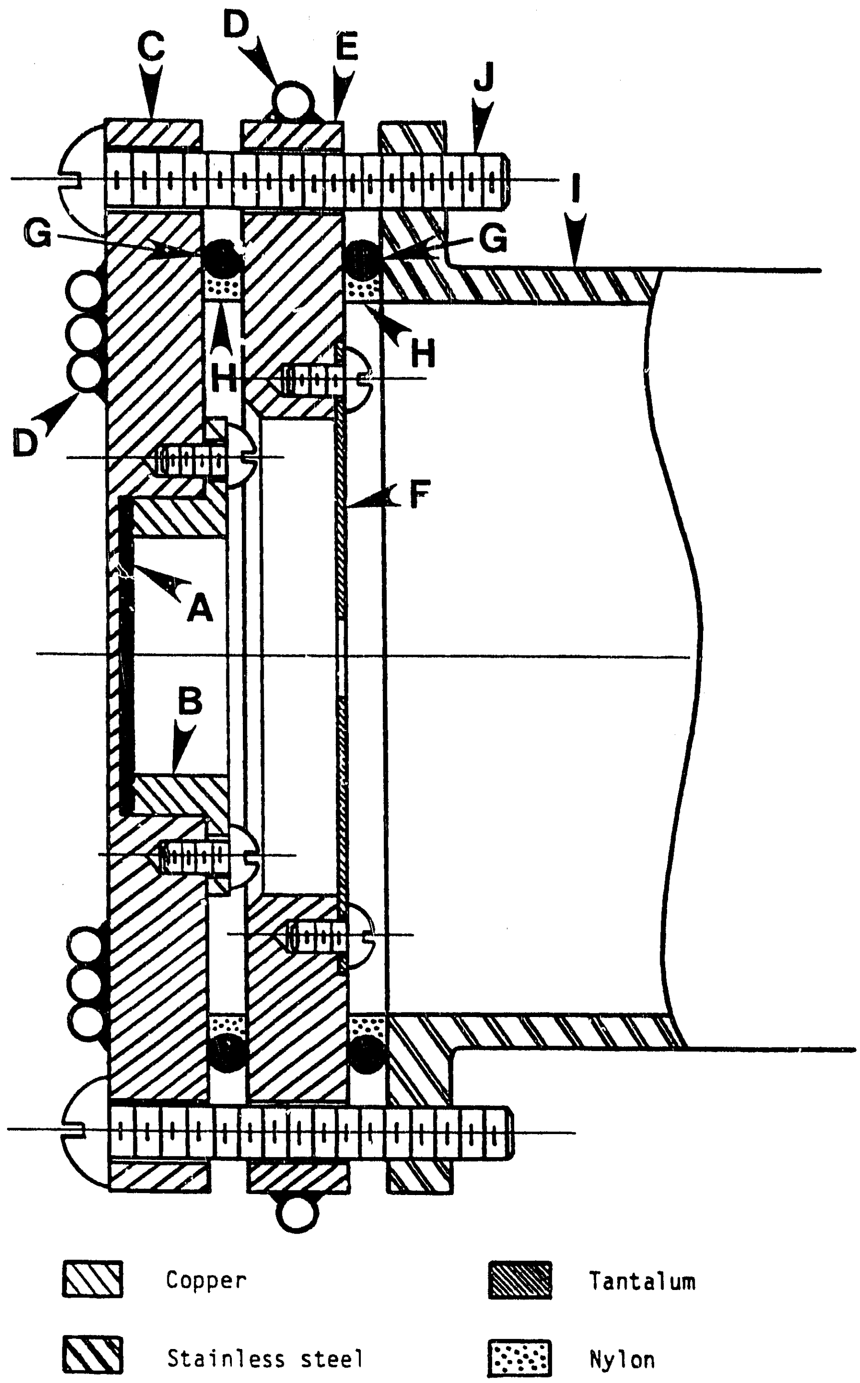

Fig. 1. A schematic drawing of the beryllium target assembly. Components are: A) Be target element. B) Be target clamp. C) Target Body. D) Copper cooling tubes. E) Aperture plate. F) Aperture. G) O-ring gasket. H) O-ring gasket spacer. I) Accelerator beam tube. J) Nylon screw.

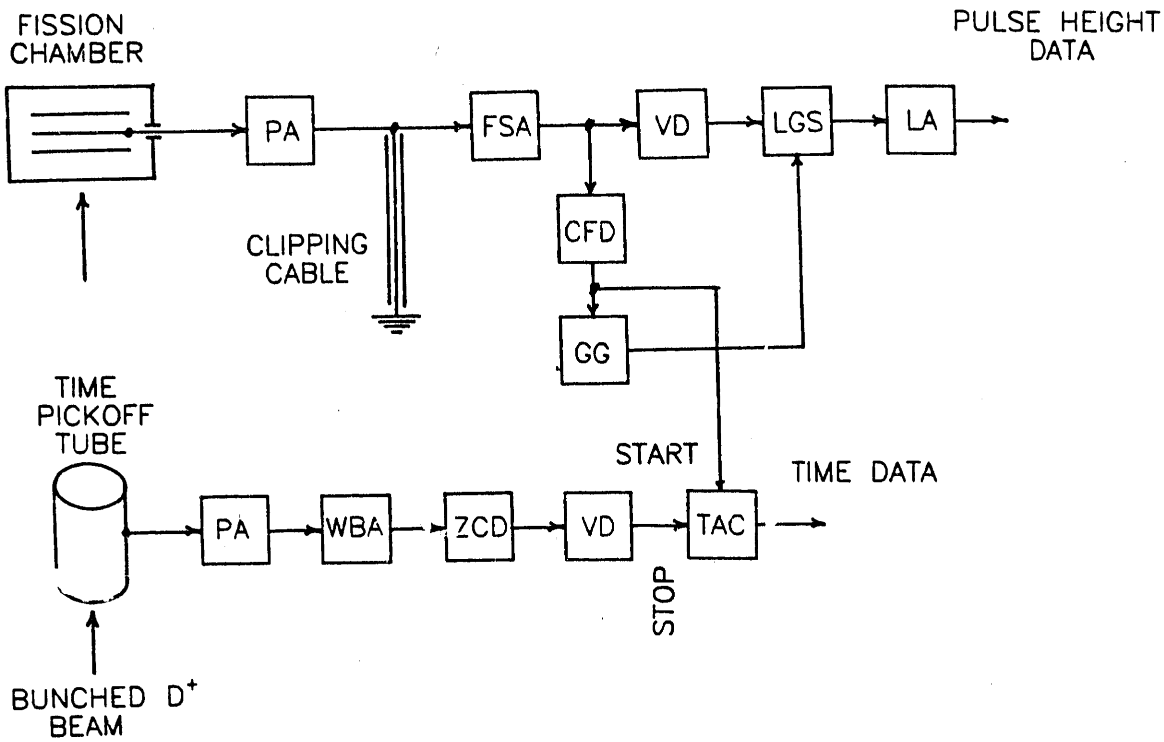

PA: Preamplifier
FSA: Fast Shaping Amplifier
CFD: Constant Fraction Discriminator
GG: Gate Generator
VD: Variable Delay
LGS: Linear Gate and Stretcher
LA: Linear Amplifier
WBA: Wide Band Amplifier
ZCD: Zero-Crossing Discriminator
TAC: Time-to Amplitude Converter

Fig. 2. The electronic circuitry used in processing events from the fission detector.

2 cm thick layer of plywood. The interior dimensions are about 1.4 m X 1.6 m X 1.9 m. The beryllium target, located near the center of the cavity, is viewed by a collimator going through the cavity wall on the zero deg. beam line. At this point, the concrete wall is 1.5 m thick. The neutron detector is placed outside the cavity. The minimum target-detector distance is 2.6 m.

The target assembly, shown in Fig. 1, is similar to the one described in ref. 11. It consists of a 25.4 mm dia. by 0.75 mm thick beryllium metal disk mounted in a copper block. The thickness of copper behind the disk is 0.75 mm. A tantalum aperture confines the deuteron beam to the center of the beryllium disk. There is a lot of material in this assembly, but most of it is in the outer regions which are not viewed by the collimator. Scattering calculations show an in-scattering effect of about 3%. To some extent, this will be spread over the entire spectrum so the effect on the shape is small.

2. Neutron Detector: The neutron detector used for the time-of-flight measurements is an ion chamber, similar to the one described in ref. 12, containing thin deposits of ^{235}U or ^{238}U. It is a low-mass, three-electrode chamber with an electrode separation of ~ 0.6 cm, and with the outer electrodes at ground potential. The center electrode is biased at + 400 V and supplies the signal. The detector is operated as a flow chamber, using high-purity methane at one atmosphere. The three electrodes are formed from four platinum disks, 70 mm dia. by 0.13 mm thick, with U_3O_8 deposits on one side. The disks are arranged so there are U_3O_8 deposits on the four-interior electrode surfaces for a total thickness of ~ 2 mg U/cm². These deposits are 50.8 mm dia. and are either ^{235}U (0.9 % ^{234}U, 93.3 % ^{235}U, 0.3 % ^{236}U and 5.5 % ^{238}U) or ^{238}U (natural uranium). Additional information on these deposits, designated U-235-J,-P, -S, -T, U-238-K, -L, -M and -O, is given in ref. 13.

The detector used for the absolute neutron yield determination had only two electrodes and contained a single 25.4 mm dia. ^{235}U deposit. The deposits used, U-235 SST-1 and SST-5, had accurately known weights and isotopic compositions[13].

The detector is operated as a current chamber, and the fast rise of the current pulse is used to provide good timing characteristics. Reference 14 provides a thorough discussion of this type of ion chamber operation. A schematic diagram of the detector system is shown in Fig. 2. The detector signal provides the START pulse to the Time-to-Amplitude converter. The beam pulse passing through a pick-up tube in the beam line near the target provides the STOP pulse. The system provides simultaneous pulse-height and time data. The time spread of the deuteron pulse at the beryllium target is believed to be < 2 nanosec and the time resolution of the gamma-detector signal for prompt gamma-rays emitted from the beryllium target is ~ 2 nanosec.

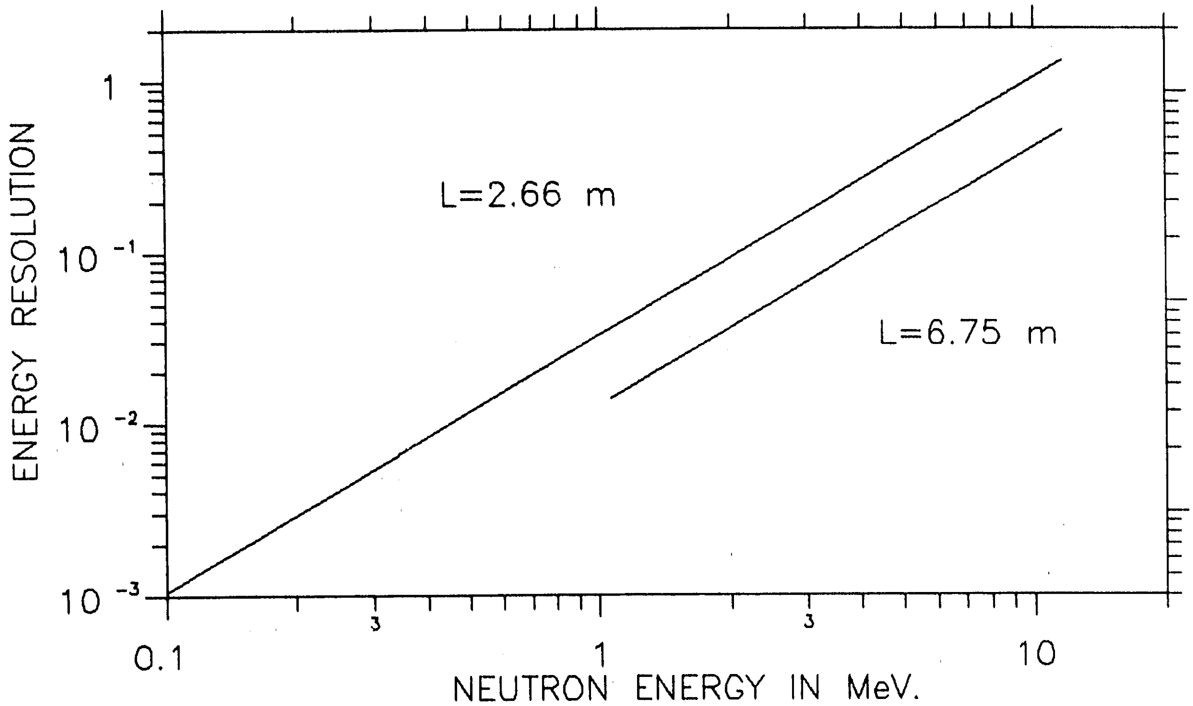

Fig. 3. The energy resolution (FWHM) for the fission detector.

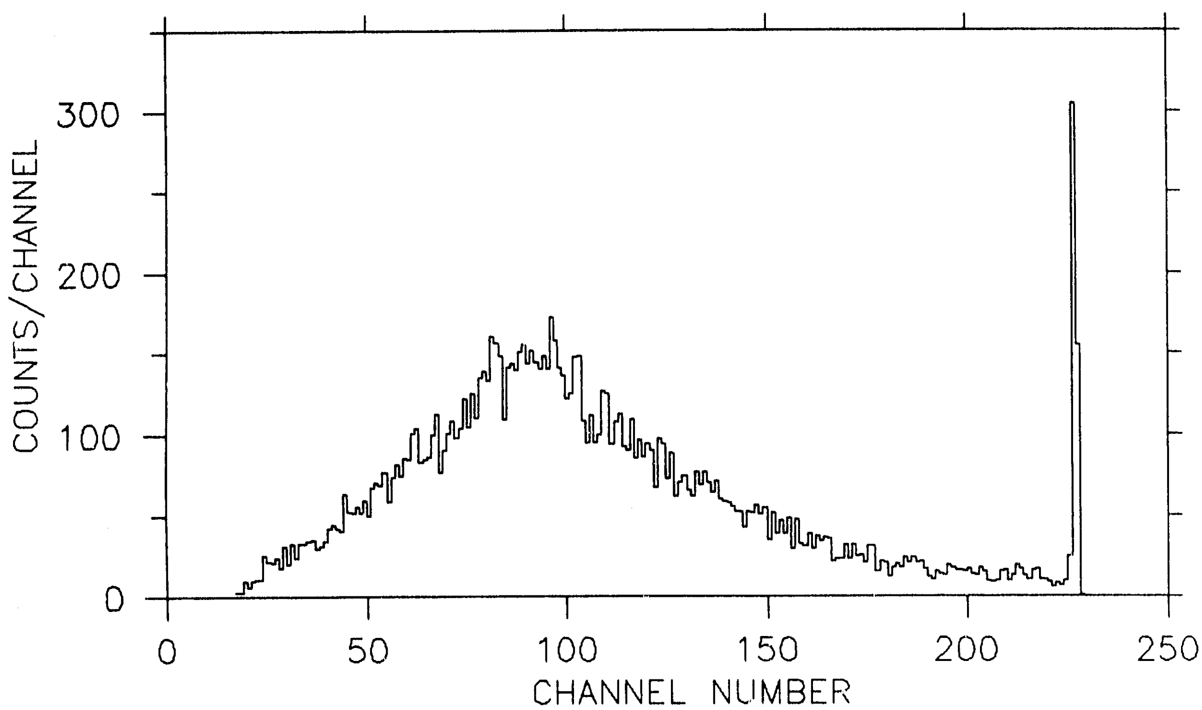

Fig. 4. A pulse-height spectrum from the ^{238}U fission chamber. The sharp peak on the right is caused by limiting in the linear-gate/stretcher.

The measured time resolution of the fission detector for monoenergetic neutrons from the $^{7}Li(p,n)$ and $D(d,n)$ reactions is ~ 3 nanosec and this is the time spread used to construct Fig. 3. The energy resolution over 7 m at the maximum neutron energy (11.4 MeV) is only ~ 0.5 MeV which limits the quality of the spectra at the highest energies. At the lower energies, the resolution is quite adequate. Even with the shortest flight path (2.66 m) the resolution at 2 MeV neutron energy is ~ 0.1 MeV.

The uranium deposits are quite thick[13] but the separation between the alphas and the fissions is fairly good. A typical pulse height spectrum is shown in Fig. 4. The sharp peak near channel 230 is an artifact introduced by the limited-dynamic range of the Linear-Gate Stretcher. The cut-off near channel 20 corresponds to the discriminator level of the Constant Fraction-Discriminator.

IV. TREATMENT OF THE DATA

Data processing for the spectral measurements involves the following steps: The neutron energy scale, based on the time calibration and the zero-time location, is determined for each measured spectrum. Measurements taken at the same deuteron energy and flight path are combined. The constant background and spectrum wraparound is subtracted and the net number of counts is determined. The analyzer time spectra are converted to energy spectra, grouped into suitable energy bins then divided by the relative detector efficiency. The relative-zero degree neutron yield was obtained by dividing each measurement at 2.66 m by the integrated deuteron beam current. Absolute neutron yields at a single energy were made using ^{235}U deposits whose masses were accurately determined.

1. Neutron Energy Scale. The determination of the energy scale requires a knowledge of the time calibration of the detector system, the distance from the neutron source to the effective center of the detector, and the energy of at least one point in the time spectrum. For the present measurement, the first two requirements were readily met. The time calibration is based on frequency measurements with an EG&G Model 462 Time Calibrator. The distance was measured directly with a metal tape.

   The third requirement is somewhat more involved. One of the usual calibration points is excluded as the neutron detector is not sensitive to gammas. However, certain features of the neutron spectra from the $^{9}Be(d,n)^{10}B$ reaction can be used to establish known energy points. One of these is the location of the maximum-neutron energy, (C_{e0}), which is the result of a transition to the ^{10}B ground state. Other important transitions are to a group of three closely-spaced levels at 5.11-, 5.16- and 5.18-MeV and to a single level at 5.92-MeV[15]. The high probability of exciting these particular levels produce prominent "edges" in the spectra which are designated C_{ei}. A good example of the association of these "edges" and levels is illustrated in

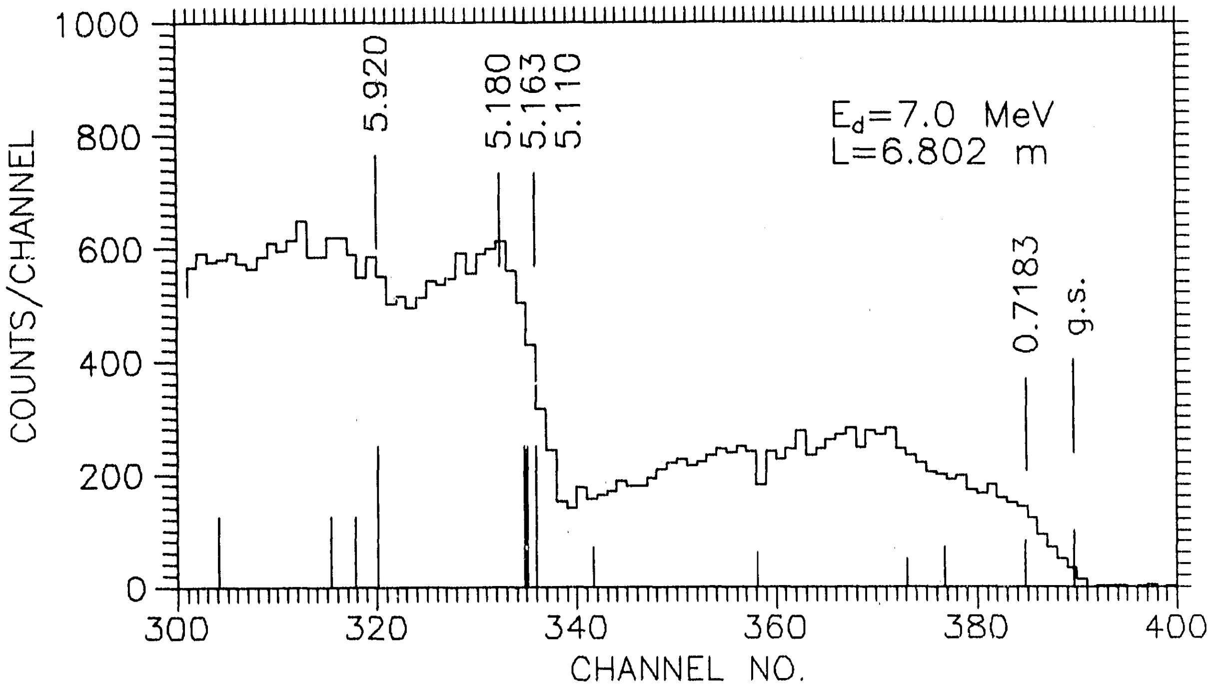

Fig. 5. A comparison of features of the thick-target Be(d,n) spectrum with energy levels in ^{10}B.

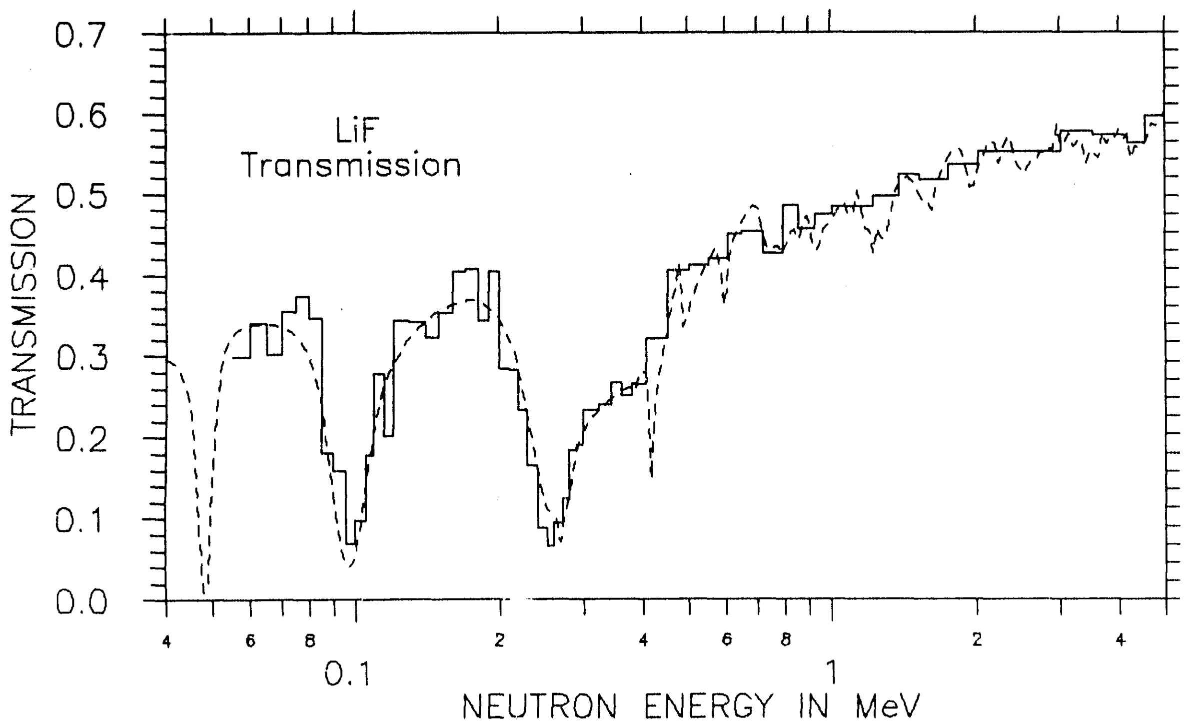

Fig 6. A comparison of the measured transmission of a LiF sample and its container with the one calculated using ENDF/B-VI cross sections.

Fig. 2 of ref. 8 where neutron-emission spectra, measured at 19 meters, for 7.5-MeV deuterons incident on thin and thick beryllium targets are compared. In the present measurement, the shorter flight paths and poorer time resolution of the detector tends to smooth some of the "edges". Still, the spectrum end-point and the more prominent edges can usually be located, and when the effect of the time resolution is taken into account, the centroid of the resonance can be accurately located. Figure 5 illustrates the correlation of some features of a spectrum from this measurement with levels in ^{10}B. A typical precision for the t=0 channel location is ~ 0.3 ns.

The Q-value for the reaction,

$$^{2}H + {}^{9}Be = n + {}^{10}B + Q_i, \tag{1}$$

leading to the i-th excited state in ^{10}B is calculated using the level information from ref. 15 and mass information from ref. 16. The laboratory energy E_{li} of a neutron emitted at 0 deg. and associated with a transition to that state is

$$E_{li}(0^o) = E_{ri} + E_c + 2.0(E_{ri}E_c)^{0.5}\cos(0^o), \tag{2}$$

where

$$E_{ri} = \left[E_d M_{be}/(M_d + M_{be}) + Q_i\right] M_{b10}/(M_n + M_{b10}), \tag{3}$$

$$E_c = E_d M_d M_n/(M_d + M_{be})/(M_n + M_{b10}). \tag{4}$$

E_c is the energy of the neutron due to the motion of the center of mass, E_{ri} is the neutron energy in the center of mass and the M_i refer to the rest masses of the particles. At the energies encountered in the present measurement, the error in E_{li} due to relativistic effects will be < 0.1 % so non-relativistic forms may be used. However, at the neutron energies of the present measurement, a non-relativistic conversion to neutron velocity may have a significant error so a relativistic calculation is used. The neutron velocity, v_{ni}, associated with each E_{li} is

$$v_{ni} = c(1 - M_n^2/(M_n + E_{li})^2)^{0.5} \tag{5}$$

where c is the velocity of light and M_n and E_{li} are in the same units. The t=0 point, C_o, is given by

$$C_o = C_{ei} + D/(v_{ni}T_n), \tag{6}$$

where D is the source-detector distance and T_n is the time per channel.

The energy scale is confirmed by locating the 260-keV lithium resonance[17], the 98-keV fluorine resonance[18] and the 430- and 1265-keV resonances in boron[19]. All these resonances have fairly low energies so their location is rather insensitive to the t=0 location. Even at 2.66 m, a shift of 1 ns corresponds to only ~ 7 keV at 1270 keV. However, the overall agreement does give confidence in the energy scale. The positions of the boron resonances were measured using a B_4C sample of undetermined thickness and served only to locate the resonance positions. The lithium and fluorine resonances were measured with a LiF sample of known thickness so the transmissions were calculated. Figure 6 compares the transmission measured over a 2.66 m flight path with that calculated using ENDF/B-VI cross sections[20].

2. Combining Measurements. The spectrum at each energy is based on a number of measurements taken under a variety of conditions and it is necessary to combine them to produce the final spectrum. The analyzer spectra are summed in their regions of overlap for measurements taken at the same deuteron energy with the same detector and over the same flight path. The summing procedure assumes that the spectrum is constant across the width of a single-analyzer channel and accounts for differences in the time-per-channel (T_c) and the t=0 position (C_o). In order to add the spectrum X_2 to spectrum X_1, the positions in X_2 corresponding to the edges of channel I in X_1 are determined. The upper edge corresponds to

$$C_{2ui} = C_{02} - (C_{01} - I)\, T_{c1}/T_{c2}. \qquad (7)$$

The lower edge corresponds to

$$C_{2di} = C_{02} - (C_{01} - I + 1)\, T_{c1}/T_{c2}. \qquad (8)$$

The C_{01} and C_{02} are the t=0 points in X_1 and X_2. Define also

$$I_u = G(C_{2ui}), \qquad (9)$$

$$I_d = G(C_{2di}), \qquad (10)$$

where G(x) is the greatest integer in x. In order to add X_2 to X_1 the number in channel I of X_1 is increased as

$$X_1(I) = X_1(I) + X_2(I_u+1)(C_{2ui} - I_u) + X_2(I_d + 1 - C_{21i}) + S, \qquad (11)$$

where

$$\begin{aligned} S &= +\sum_{I_d+2}^{I_u} X_2(I_i) \qquad &\text{for } I_u - (I_d+2) > 0 \\ S &= 0 \qquad &\text{for } I_u - (I_d+2) \leq 0 \end{aligned} \qquad (12)$$

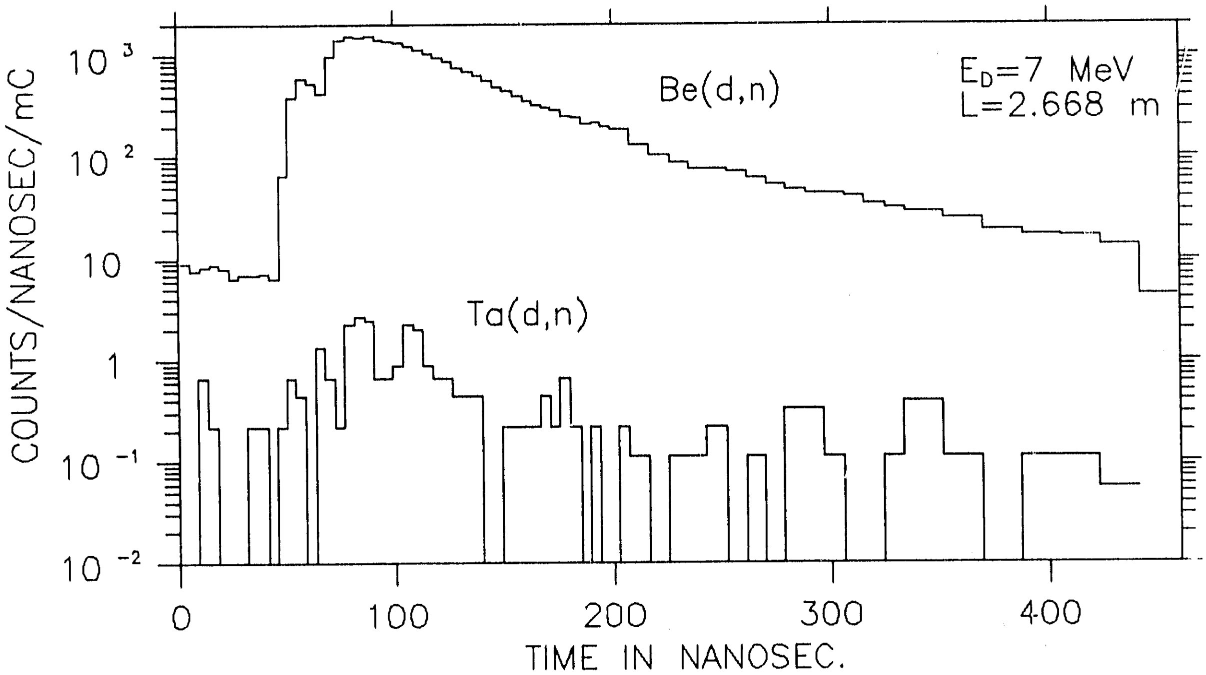

Fig. 7. A comparison of neutron yield and spectra from thick beryllium and tantalum metal targets.

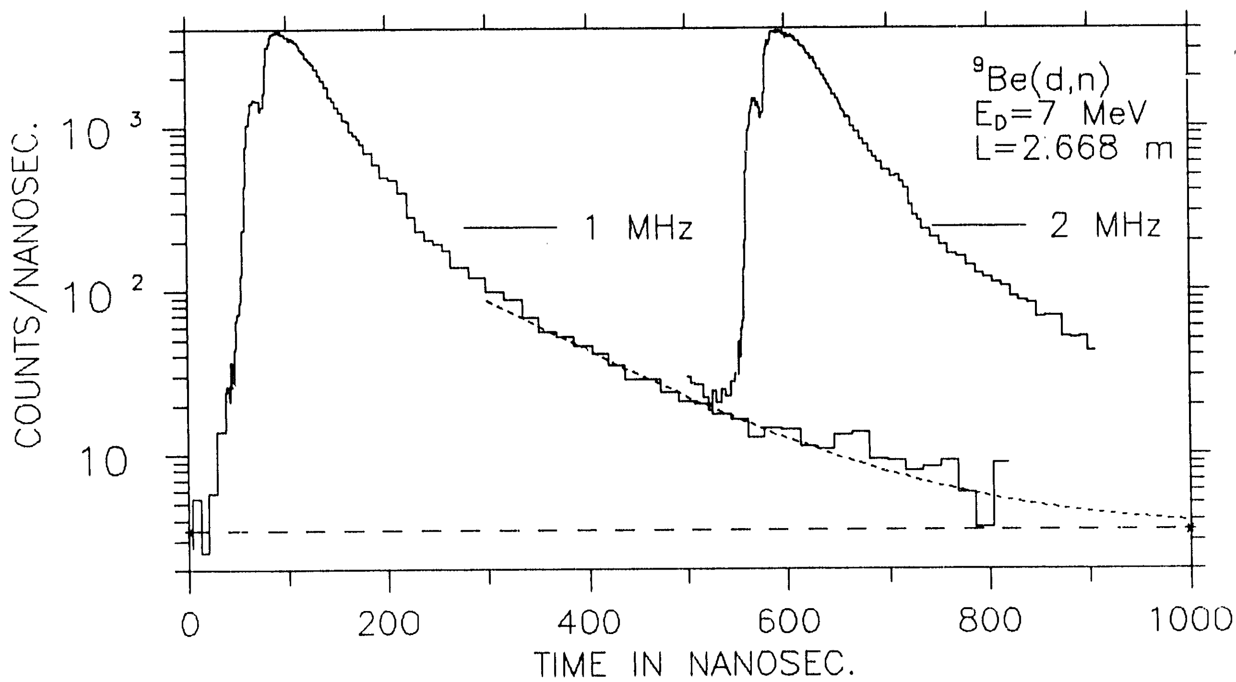

Fig. 8. Thick Be-target-spectra for 7-MeV deuteron energy measured with 1 and 2 MHz repetition rates normalized to the same integrated deuteron current. The curved dasked line is eq. (13) fitted to the 1-MHz above 300 nanosec. The horizonal line is A of eq. 13.

This continues for all I in X_1 where I_u and I_d are within the range of X_2.

The above procedure can only be used in the region where the spectra overlap. It was also necessary to combine spectra outside the overlap region. For example, the 2-MHz measurements only cover the neutron-energy region above ~ 0.25-MeV. Lower energies, down to ~ 0.050-MeV are covered by the 1-Mhz measurements. The 0.050 - 0.25-MeV region of the 1-MHz data is combined with the 2-MHz data through their energy spectra. The energy-bin structure of the two spectra are adjusted so they are similar in the vicinity of 0.25-MeV and the spectra are then normalized. The final spectrum uses the 1-MHz data below 0.25-MeV and the 2-MHz data above that energy.

The measurements with the ^{235}U detector at 2.66 m and with the ^{238}U detector at 6.75 m are also combined through the energy spectra. The energy bin structure of the spectra are adjusted so they are similar in the vicinity of 2.5-MeV neutron energy and the two spectra are normalized so that their integrals above 2.5-MeV are equal. The final spectra uses the ^{235}U measurement at 2.66 m below 2.5-MeV and the ^{238}U measurement above 2.5-MeV.

3. Background corrections: Since the detector is at zero deg. and the collimator looks down the flight tube, neutrons produced at the beam-pulse-pick-off tube, slits and cold trap will be detected. However, the thick beryllium target is such a prolific neutron source that these secondary sources should be negligible. In order to see if these neutrons are a significant problem, the neutron spectrum of a tantalum target is compared with that of a beryllium target. The results are shown in Fig. 7. As expected, the yield of the tantalum target plus any secondary neutron sources is no more than 1% of the beryllium target yield.

The principle correction to the data is due to the spectrum wraparound. In principal, the neutron spectrum can extend to near zero energy and the ^{235}U chamber will detect these neutrons with increasing efficiency for lower energies. Thus, the primary spectrum sits on the tails of the spectra from earlier beam pulses. Figure 8 shows plots of spectra measured with 500 and 1000 nanosec periods that are normalized to the integrated deuteron current. The short period spectrum appears to sit very nicely on the tail of the previous pulse.

The low-energy parts of these spectra are very similar for all deuteron energies, and for times longer than about 300 nanosec, are described very well by

$$N(t) = A + Be^{-Ct}. \qquad (13)$$

Time distributions were measured with the ^{235}U detector for a target-detector distance of 2.7 m and a pulse-repetition rate of 1 MHz at several incident deuteron energies. The spectra were

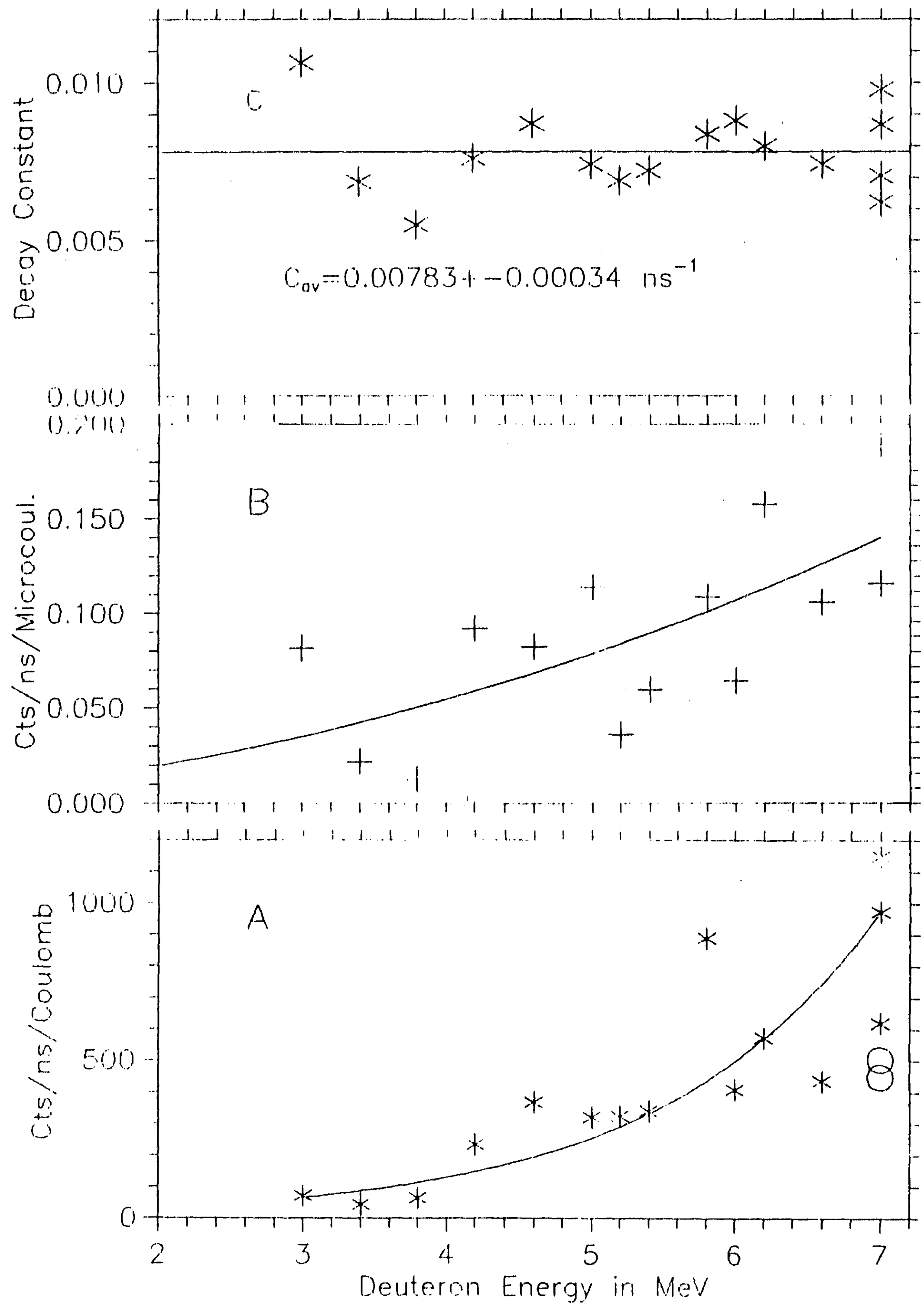

Fig. 9. The parameters of eq. (13) as a function of deuteron energy. The o are values of A based on with the collimator plugged or with the detector moved to one side of the opening.

fit by the above equation with the results shown in Fig. 9. The value of C is essentially independent of deuteron energy and has an average value of 0.00783 ± 0.00034 ns^{-1}. The value of C should be inversely proportional to the target-detector separation distance, and measurements at 3.7 m confirmed this. The values of A and B scatter widely, but do decrease with deuteron energy. The curves through the data are the results of fits to the data, with the restriction that B go to zero at zero deuteron energy.

The wraparound correction is based on eq. (13) and the values of A, B and C given by the curves in Fig. 9. The values of A and B were scaled as necessary so that the N(t) fit the observed neutron yield above the high-energy end of the spectrum. In Fig. 8, this is the region between 500 and 550 nanosec. (Note that the time, t, is referenced to t=0 for the previous neutron pulse.) Figure 8 also shows that the wraparound correction for the 1-MHz measurements is smaller as the time dependent term has almost disappeared when the next neutron pulse occurs. However, going to 1-MHz doubles the time required for the measurement so 2-Mhz is used for most of the work above 0.25-MeV.

Only the B term in eq. (13) is due to spectrum wraparound. Much of the constant term is produced by room return neutrons and by leakage through the cavity walls. At 7-MeV deuteron energy, measurements of the background were made with the collimator plugged and also with the detector moved to one side of the collimator opening. The results of the two measurements, also shown in Fig. 9, are in agreement but are much less than the value of A determined by the fit to the spectra. However, they are fairly consistent with the lower energy values.

The possibility that there were a significant number of low-energy neutrons streaming through the collimator was also considered. However a measurement made through a collimator at about 80 deg. to the beam axis that looked at a point in the source cavity about 15 cm downstream from the target showed no difference in the count rate with the collimator open and plugged.

Although the wraparound correction is a significant one, it is not enormous over most of the spectrum. At 0.060-MeV neutron energy and 1-MHz, it is typically 50% ,but it decreases rapidly with increasing neutron energy. At 0.25-MeV and 2 Mhz, the correction is 10 - 15 %, but over much of the spectrum it is no more than 1%.

4. <u>Conversion of Time Spectra to Energy Spectra.</u> The convention employed in this work assumes that the analyzer channel number C_j is associated with the upper edge of channel j. However, C_0 refers to the location of the zero-time point within a channel. Thus, the maximum velocity of a neutron detected in channel j is

$$v_j = \frac{D}{T_n(C_o - C_j)} . \quad (14)$$

The corresponding laboratory neutron energy is

$$E_j = M_n((1 - v_j^2/c^2)^{-0.5} - 1). \quad (15)$$

The number of counts in the jth analyzer channel, $N(C_j)$, is converted to counts per unit energy, $N(E_j)$, by

$$N(E_j) = N(C_j)/(E_j - E_{j-1}). \quad (16)$$

5. Source Yield. The measurement of the source yield was made with a fission chamber containing a ^{235}U deposit of known isotopic composition and weight in a known geometry. The total fissions are corrected for losses below the discriminator setting, losses in the deposits, transmission through any intervening material and for scattering into the deposits. This corrected fission count is related to the neutron yield and spectrum and to the fission cross section by

$$Y_f = 2\pi I_n F G N \int_0^{E_u} \int_0^{\theta_u} P(E,\theta)\sigma(E)\sin(\theta)d\theta dE \quad (17)$$

where I_n is the number of neutrons/sr/μcoulomb at 0 deg., F is the integrated deuteron current in μcoulomb, G is the geometry factor, N is the atoms U/cm^2, $P(E,\theta)$ is the normalized energy and angle dependent neutron spectrum and $\sigma(E)$ is the fission cross section. If θ_u is small, then $P(E,\theta)$ becomes essentially independent of θ and eq. (12) becomes

$$Y_f = 2 \pi I_n F G N \Omega \langle\sigma\rangle \quad (18)$$

here Ω is the solid angle in sr and $\langle\sigma\rangle$ is the fission cross section averaged over the zero deg. spectrum.

Relative yield measurements with the ^{235}U detector were made at 2.6 m where θ_u was only 0.5 deg. Absolute measurements were made inside the source cavity at 7-MeV deuteron energy using ^{235}U deposits of known weight and isotopic composition. In order to reduce the error due to the uncertainty in the solid angle, several distances were used and θ_u ranged from 3 to 5.5 deg. Equation (18) should still be valid. The relative measurements are normalized to this value.

Figure 10 shows the time correlation of fission events for a ^{235}U detector inside the cavity. The time-independent background is due to neutrons which have lost most of their energy by multiple scattering in the cavity walls and structure. The peak is due to neutrons which come directly from the neutron source. The time correlation of the fissions with the deuteron

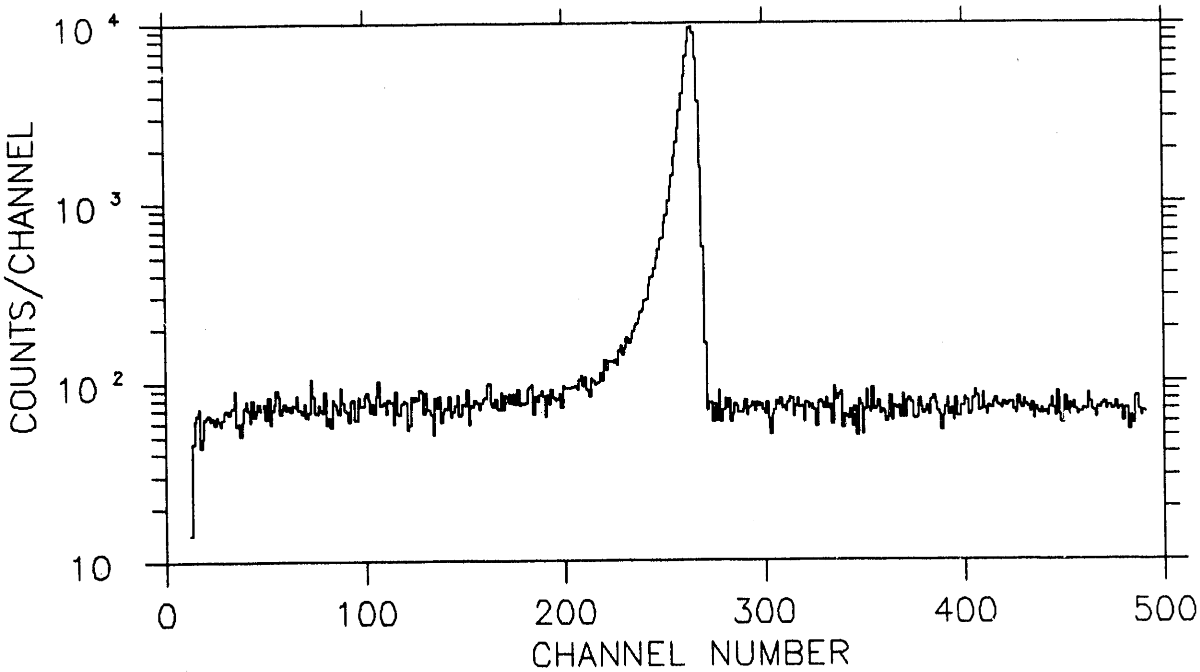

Fig. 10. The time-correlated fission events for a ^{235}U detector inside the source cavity at a distance of 17 cm.

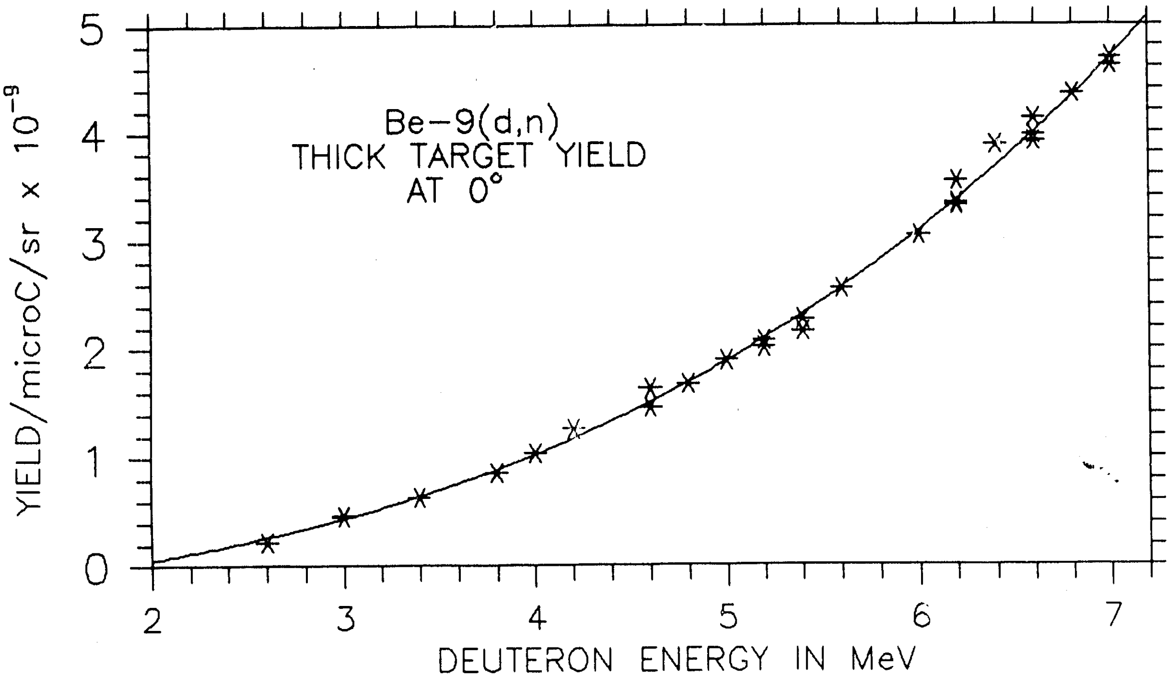

Fig. 11. The Be(d,n) thick-target yield at 0 deg. The data points are relative measurements. The curve is a fit to the data normalized to an absolute measurement at 7.0 MeV deuteron energy.

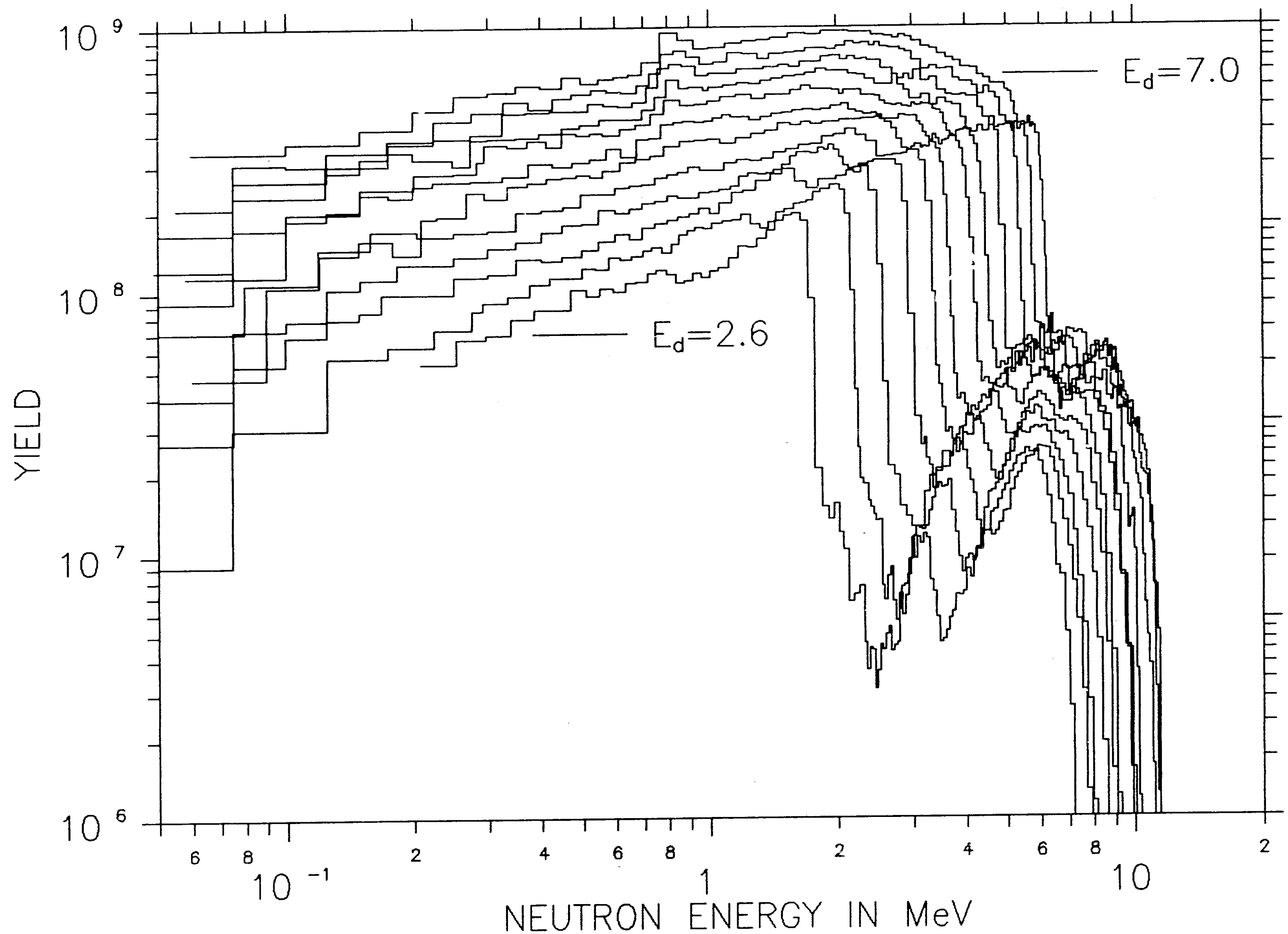

Fig. 12. A summary of the $^{9}Be(d,n)$ thick target yields at 0 deg. as a function of E_d and E_n.

beam pulse permits a clear separation of the two groups. The fission counts in the peak were corrected for losses[19] below the discriminator setting, losses in the deposit and for scattering and transmission in the source and detector structures.

V. RESULTS

The total zero deg. neutron yield is shown in Fig. 11. The data points shown are the results of relative measurements that are normalized to the absolute measurement at 7.0-MeV deuteron energy as described in Section IV-5. This gives 4.66×10^9 neutrons/sr/μC which is in fair agreement with the results of Lone et al[5] and Weaver et al[2].The curve is a 3rd-order polynomial that fits the data. The yield between 2.6- and 7.0-MeV deuteron energy is given by

$$Y_n(E_d) = 10^9 \times (-0.3819 + 0.1740E_d - 0.00137E_d^2 + 0.01131\, E_d^3) \qquad (19)$$

where Y_n is in units of neutrons/sr/μC and E_d is in MeV.

The total-systematic error in the neutron yield is 4.0%. The principal contributors are geometry factor, 0.6 %, uranium sample weight, 0.5 %, detector efficiency corrections, 0.5 %, scattering and transmission corrections, 1.1 %, room return background correction, 1.0 %, deuteron charge measurement, 2.0 % and ^{235}U cross section, 3.0 %.

Figure 12 summarizes the spectral distributions and yields observed at zero deg. from the thick-target Be(d,n) reaction at deuteron energies of 2.6 to 7.0-MeV. For deuteron energies of 5.8- through 7.0-MeV, the spectra above 2.5-MeV neutron energy are based on measurements with the ^{238}U detector at 6.75 m. For neutron energies below 2.5-MeV, and for all other deuteron energies, they are derived from measurements with the ^{235}U detector at 2.66 m. Most of these measurements were made with a time/channel of ~ 0.9 nanosec. At the highest energies, each energy bin corresponds to a single analyzer channel, or about a third of the actual energy resolution. At the lower energies, each energy bin corresponds to a sum over many analyzer channels. The bin structure is not consistent at all deuteron energies. In Appendix A these results are given as individual graphs and Tables.

The spectra presented here are the spectra of neutrons emitted at zero deg. for this particular source assembly. The only correction applied to the data that affects the shape of the spectra is the removal of the background discussed in Section IV-3. They have not been corrected for in-scattering by the target assembly or for transmission through the target assembly and the neutron detector wall. The transmission factor for the ^{235}U detector, averaged over the 7-MeV spectrum is 0.964. The energy dependence of the total cross sections causes more lower-energy neutrons to be removed than

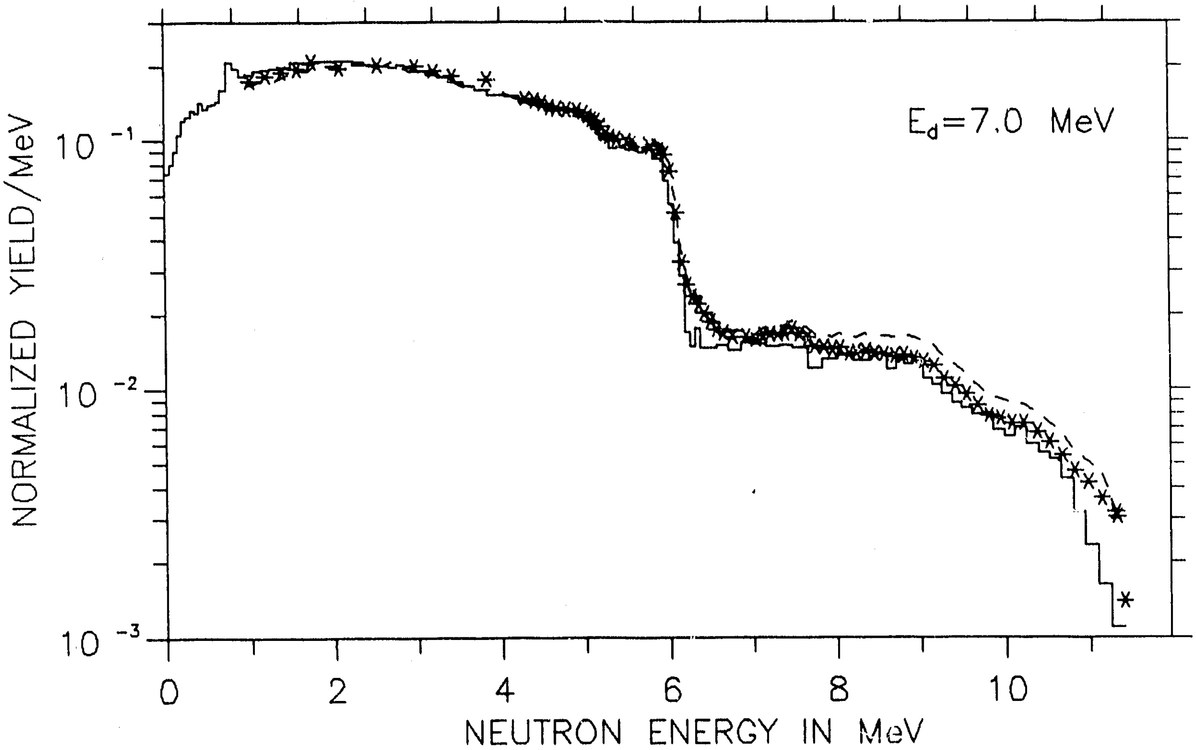

Fig. 13. A comparison of the spectrum at 7.0 MeV deuteron energy with the data of Crametz et al[6] (– – –) and with the modified spectrum of Smith and Greenwood[20] (***). All spectra have the same normalization.

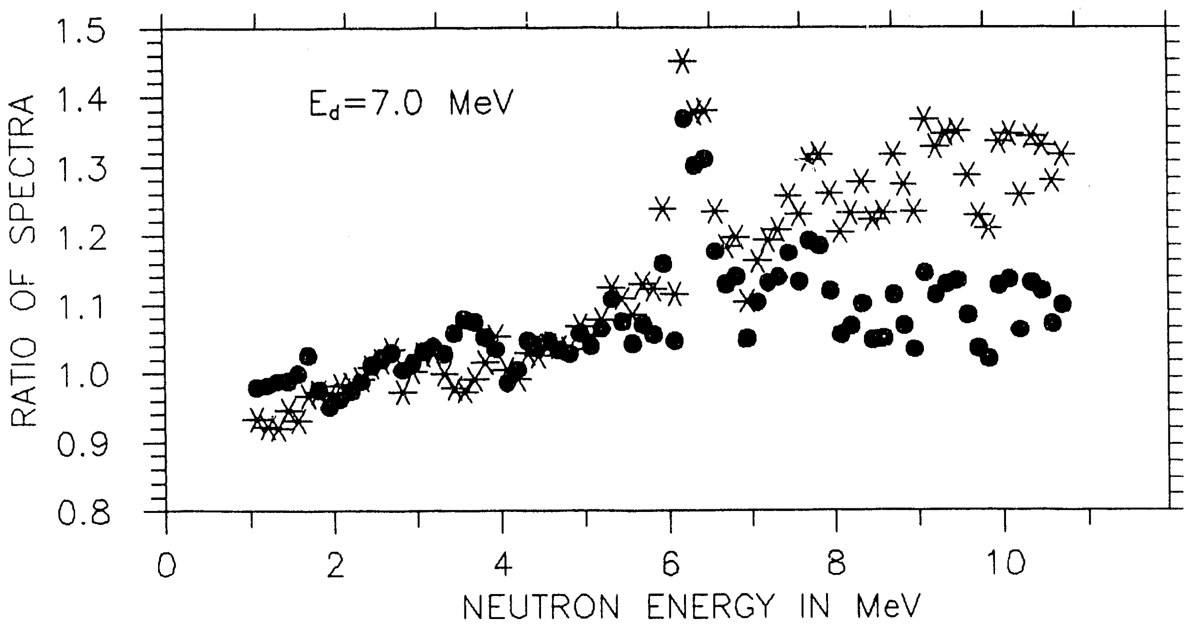

Fig. 14. The ratio of the spectrum in Fig. 13 to the data of Crametz et al[6] (***) and Smith and Greenwood[20] (●●●).

higher-energy ones. The in-scattering factor for the source assembly minus the beryllium-metal disk when the ^{235}U detector is used is 1.027. About half is inelastic scattering, so this effect tends to add neutrons to the lower-energy region. The two effects are of similar magnitude and tend to cancel. Complete cancellation of the effect of the spectrum shape is unlikely as the energy dependence of the total cross sections is not very strong. There may also be some scattering from the collimator, although earlier tests in different experimental set-ups with mono-energetic neutron sources did not show a significant effect. The spectra from the present source assembly should not be greatly different from the true-reaction spectra. However, it is conceivable that the spectra from another assembly could differ significantly.

At all deuteron energies, most of the neutron yield appears to be due to stripping reactions leading to levels in ^{10}B around 5.2- and 5.9-MeV excitation. (See Fig. 5.) The higher-energy portions of the spectra are due to reactions leading to lower-lying levels in ^{10}B. Below ~ 0.6-MeV, all the spectra show a similar behavior and decrease linearly with $\ln(E_n)$. Above 5.4-MeV deuteron energy, all spectra show a well defined peak at ~ 0.8-MeV. This phenomena was observed earlier by Lone et al [4,5] who attributed it to the excitation of the 2.43-MeV level in ^{9}Be by an inelastic process followed by the decay of that level to ^{8}Be by neutron emission.

Crametz, Knitter and Smith[6] have reported a detailed measurement of the 7-MeV Be(d,n) spectrum which has often been used for nuclear data studies. Smith et al[21] have used the code STAYSL to adjust the spectrum to give the most consistent results with a set of well-determined dosimetry reactions. These spectra, normalized to 1.0, are compared with the present result in Fig. 13. A better comparison is shown in Fig. 14, where the ratio to the present 7-MeV measurement is shown. Below 6-MeV, both ratios are near 1.0 but they diverge above 7-MeV. The principal effect of the adjustment with STAYSL was to reduce the yield in this region, and the adjusted spectrum was in much better agreement with the present measurement. There is a prominent spike in the ratios between 6- and 7-MeV. Inspection of the spectra in Fig. 13 shows obvious differences which may be due in part to such things as small differences in energy resolution and energy scale. Also, the ^{238}U fission-cross section is changing rapidly in that region.

The average-neutron energy is computed for all spectra and is found to be linear with E_d as shown in Fig. 15. For the deuteron-energy range of these measurements, the average neutron energy, $\langle E_n \rangle$, can be estimated from the following expression:

$$\langle E_n \rangle = (1.210 + 0.277 E_d)\,\text{MeV} \qquad (20)$$

These average energies are in fair agreement with those reported by Lone et al[5], although systematically about 0.2-MeV larger.

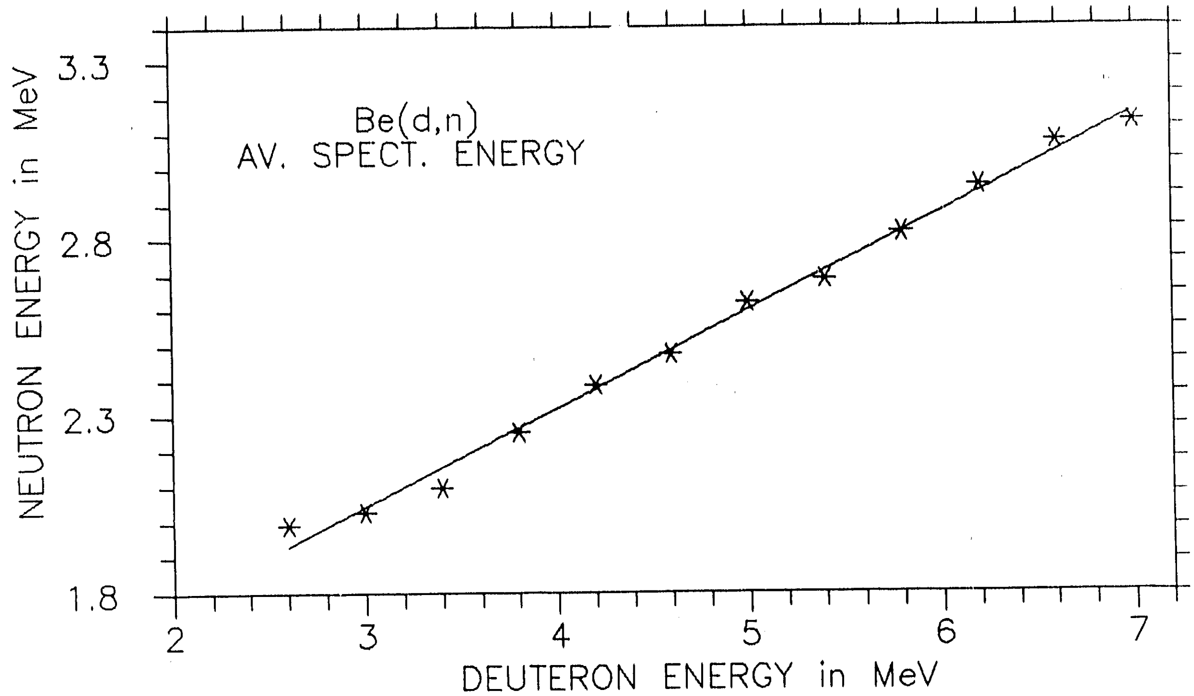

Fig. 15. The average neutron energy as a function of the incident deuteron energy.

ACKNOWLEDGMENTS

This work was supported by the U. S. Department of Energy under contract W-31-109-Eng-38. The author is indebted to J. J. Fabish, D. L. Smith, V. Svirtun and R. R. Whitman for their assistance in the acquisition and interpretation of this data.

REFERENCES

1. D. L. Smith, "A Least-Squares Method for Deriving Reaction Differential Cross Section Information from Measurements Performed in Diverse Neutron Fields", ANL/NDM-77, Argonne National Laboratory (1982).

2. K. A. Weaver, J. D. Anderson, H. H. Barschall and J. C. Davis, Nucl. Sci. Eng. 52, 35-45 (1973).

3. Yong Sook Park, A. Niiler and R. A. Lindgren, Phys. Rev. C8, 1557(1973).

4. M. A. Lone and B. C. Robertson, Proc. Symp. on Neutron Cross-Sections from 10-50 MeV, National Nuclear Data Center, Brookhaven National Laboratory, U.S.A. Report BNL-NCS-51245 (1980).

5. M. A. Lone, A. J. Ferguson and B. C. Robertson, Nucl. Instr. Methods 189, 515-523 (1981).

6. A. Crametz, H. -H. Knitter and D. L. Smith, "Thick-Target $^{9}Be(d,n)^{10}B$ Neutron Spectrum at E_d=7 MeV", Nuclear Data for Science and Technology, edited by K. H. Boeckhoff, D. Reidel Publishing Company, Dordrecht, Holland (1983), p. 902.

7. D. L. Smith, J. W. Meadows and P. T. Guenther, Nucl. Instr. Methods A241, 507-510 (1985). See also "Fast-Neutron-Spectrum Measurements for the Thick-Target $^{9}Be(d,n)^{10}B$ Reaction at E_d = 7 MeV", ANL/NDM-90, Argonne National Laboratory (1985).

8. F. M. Baumann, G. Domogala, H. Freiesleben, H. J. Paul, S. Puhlvers and H. Sohlbach, Nucl. Instr. Methods A247, 359-366 (1986).

9. H. J. Brede, G. Dietze, K. Kudo, U. J. Schrewe, F. Tancu and C. Wen, Nucl. Instr. Methods A274, 332-344 (1989).

10. J. W. Meadows, "Determination of the Energy Scale for Neutron Cross Section Measurements employing a Monoenergetic Accelerator", ANL/NDM-25, Argonne National Laboratory (1977).

11. Donald L. Smith and James W. Meadows, "A Facility for High-Intensity Neutron Irradiations using Thick-Target Sources at the Argonne Fast Neutron Generator", ANL/NDM-95, Argonne National Laboratory (1986).

12. J. W. Meadows, "The Fission Cross Sections of Some Thorium, Uranium, Neptunium and Plutonium Isotopes Relative to ^{235}U", ANL/NDM-83, Argonne National Laboratory (1983).

13. J. W. Meadows, "Characteristics of Samples in the FNG Fission Deposit Collection", ANL/NDM-118, Argonne National Laboratory (1990).

14. C. Budtz-Jørgensen and H.-H. Knitter, Nucl. Sci. Eng. 79, 380 (1981).

15. C. Michael Lederer and Virginia S. Shirley, editors, Table of Isotopes, 7th Edition, John Wiley & Sons, New York, NY (1978).

16. Nuclear Wallet Cards, Jagdish K. Tuli, U.S. National Nuclear Data Center, Brookhaven National Laboratory, Upton, New York (1990).

17. J. W. Meadows and J. F. Whalen, Nucl. Sci. Eng. 41,351-356 (1970).

18. U. N. Singh, H. I. Liou, J. Rainwater, G. Hacken and J. B. Garg, Phys. Rev. C10, 2147-2149 (1974).

19. S. F. Mughabghab, M. Divadeenam, and D. I. Garber, Neutron Cross Sections, Volume I, Resonance Parameters and Thermal Cross Sections, Part A, Z = 1 - 60, Academic Press, Inc., New York, NY (1948).

20. ENDF/B-VI (1990) Evaluated Nuclear Data File, ENDF/B, Version VI, National Nuclear Data Center, Brookhaven National Laboratory, Upton, NY, 11973, U.S.A.

21. D. L. Smith, J. W. Meadows and L. R. Greenwood, Proc. 7th ASTM-Euratom Symposium on Reactor Dosimetry, Strasbourg, France, 27-31 August 1990, eds. R. Dierckx and W. N. McElroy (1990).

APPENDIX A

YIELD AND ENERGY DISTRIBUTION TABLES

The yield and energy distributions for zero deg. neutron emission from the thick-target Be(d,n) reaction as a function of the incident deuteron energy is given in the form

$$N(E_d,E_n,0) = Y_n(E_d,0)\ P(E_d,E_n,0)$$

where $Y_n(E_d,0)$ is the total zero deg. yield in neutrons/sr/μC as a function of the incident deuteron energy. $P(E_d,E_n,0)$ is the normalized distribution in neutron energy at zero deg. $Y_n(E_d,0)$ is listed in Table A-I. It is calculated from a polynomial fit to the experimental data using eq. (19) and is illustrated in Fig. 11. $P(E_d,E_n,0)$ is listed in Tables A-II through A-XIII and is illustrated by Figs. A-1 through A-12.

In Tables A-II through A-XII the energy columns give the energy of the upper edge of the energy bin with the exception of the first entry which gives the energy of the lower edge of the first bin. The yield columns give the normalized yield/MeV. The error columns include only the statistical counting errors.

Table A-I. $Y_n(E_d,0)$, the zero deg. neutron yield from the Be(d,n) reaction as neutrons/sr/μC. The estimated systematic error is 4.0 %.

E_d MeV	$Y_n(E_d,0)$ n/sr/μC
2.6	0.262×10^9
3.0	0.435
3.4	0.641
3.8	0.883
4.2	1.167
4.6	1.495
5.0	1.873
5.4	2.305
5.8	2.796
6.2	3.349
6.6	3.968
7.0	4.660

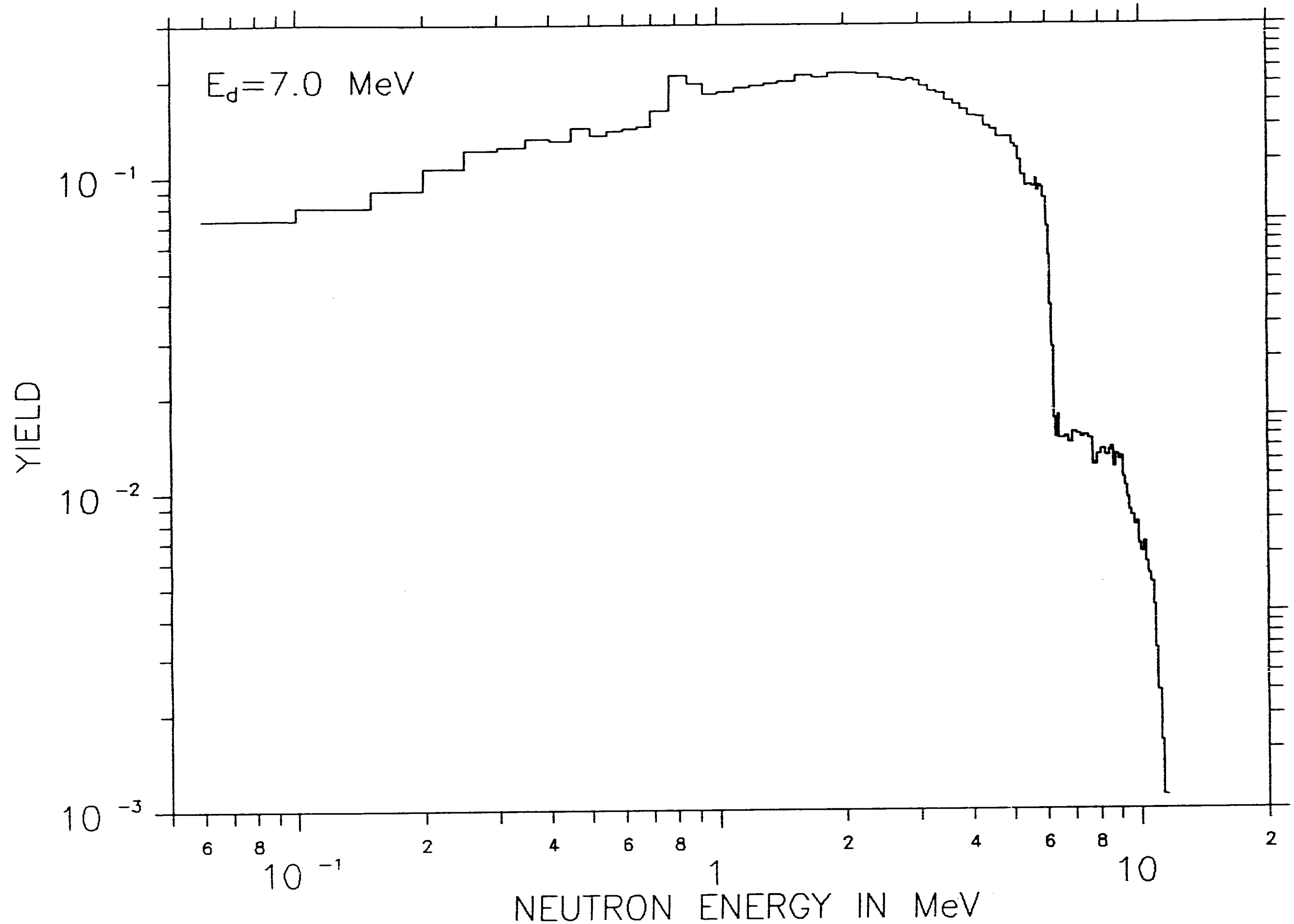

Fig. A-1. The normalized spectrum of neutrons emitted at 0 deg. with respect to 7.0 MeV deuterons incident on a thick Be-metal target.

Table A-II. The normalized zero deg. neutron emission spectrum for 7.0 MeV deuterons on a thick Beryllium metal target.

Upper Edge MeV	Yield per MeV	Stat Err %	Upper Edge MeV	Yield per MeV	Stat Err %	Upper Edge MeV	Yield per MeV	Stat Err %
.0594	----	---	3.1680	.1887	1.7	6.9078	.0140	4.3
.0999	.0725	2.5	3.3087	.1814	1.8	7.0568	.0152	4.0
.1505	.0792	2.7	3.4590	.1780	1.7	7.2108	.0150	3.9
.2001	.0891	2.9	3.6197	.1688	1.7	7.3698	.0146	3.9
.2497	.1047	2.4	3.7625	.1637	1.8	7.5342	.0148	3.7
.3002	.1191	2.0	3.9138	.1584	1.8	7.7042	.0145	3.7
.3502	.1223	2.1	4.1079	.1507	1.6	7.8800	.0120	3.9
.3997	.1301	2.0	4.2808	.1496	1.7	8.0620	.0130	3.7
.4495	.1274	2.1	4.4272	.1400	1.9	8.2504	.0135	3.6
.4996	.1398	2.0	4.5812	.1363	1.9	8.4454	.0128	3.7
.5473	.1323	2.1	4.7021	.1301	2.1	8.5456	.0133	4.3
.5981	.1368	2.0	4.8279	.1300	2.1	8.6476	.0136	4.3
.6468	.1391	2.1	4.9588	.1295	2.0	8.7514	.0118	4.4
.6964	.1416	2.0	5.0490	.1231	2.4	8.8571	.0130	4.4
.7700	.1586	1.6	5.1418	.1200	2.3	8.9647	.0125	4.3
.8487	.2056	1.4	5.2371	.1094	2.4	9.0743	.0127	4.3
.9239	.1921	1.4	5.3351	.0986	2.5	9.1860	.0109	4.4
1.0005	.1791	1.4	5.4359	.0914	2.6	9.2997	.0103	4.6
1.0973	.1808	1.3	5.5396	.0922	2.5	9.4156	.0094	4.7
1.1970	.1874	1.2	5.6463	.0908	2.5	9.5337	.0086	4.9
1.2976	.1902	1.2	5.7008	.0962	3.0	9.6540	.0083	5.0
1.3963	.1931	1.2	5.7561	.0880	3.0	9.7766	.0078	5.1
1.5407	.1957	1.0	5.8122	.0914	3.0	9.9016	.0079	5.1
1.6887	.2043	.9	5.8692	.0898	2.9	10.0290	.0068	5.2
1.8365	.2024	.9	5.9856	.0834	2.4	10.1590	.0064	5.4
1.9793	.2073	.9	6.0452	.0678	3.1	10.2910	.0069	5.4
2.1393	.2076	.9	6.1056	.0550	3.3	10.4260	.0059	5.4
2.2881	.2065	.9	6.1670	.0383	3.7	10.5640	.0054	5.7
2.4185	.2060	.9	6.2292	.0283	4.2	10.7050	.0051	5.8
2.6001	.1996	2.2	6.2925	.0167	5.0	10.8480	.0043	6.1
2.7223	.1974	1.8	6.3567	.0146	5.8	10.9950	.0032	6.8
2.8149	.1953	2.1	6.4219	.0173	5.6	11.1440	.0023	7.9
2.9124	.1993	2.0	6.4881	.0145	5.5	11.2960	.0016	9.2
3.0150	.1955	2.0	6.6236	.0144	4.5	11.4520	.0011	10.9
3.1680	.1887	1.7	6.7635	.0147	4.3	11.6110	.0004	14.5

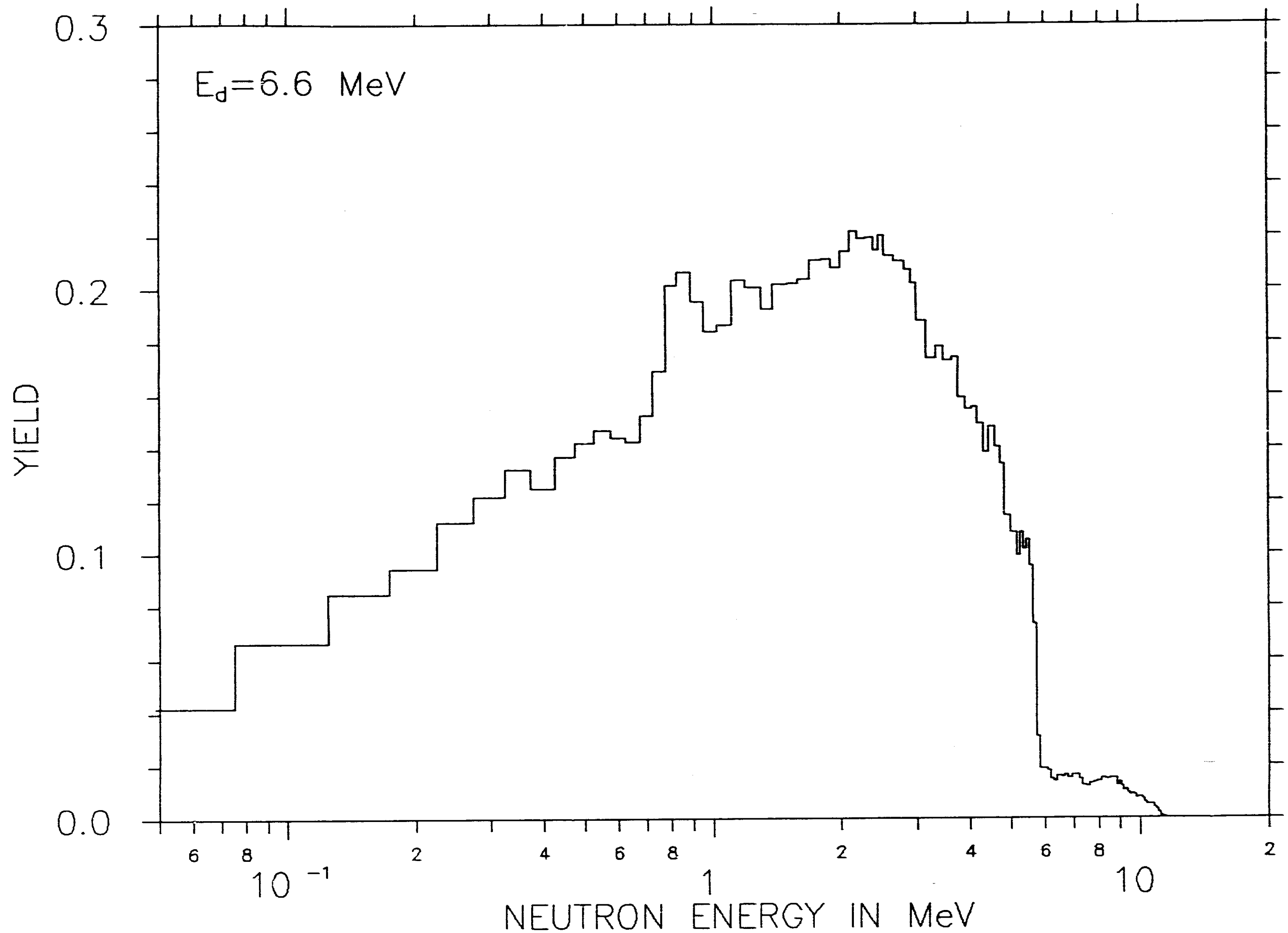

Fig. A-2. The normalized spectrum of neutrons emitted at 0 deg. with respect to 6.6 MeV deuterons incident on a thick Be-metal target.

Table A-III. The normalized zero deg. neutron emission spectrum for 6.6-MeV deuterons on a thick Beryllium metal target.

Upper Edge MeV	Yield per MeV	Stat Err %	Upper Edge MeV	Yield per MeV	Stat Err %	Upper Edge MeV	Yield per MeV	Stat Err %
.0490	----	---	2.6555	.2125	1.8	7.1685	.0162	4.0
.0750	.0417	3.0	2.8226	.2105	1.6	7.3129	.0149	4.0
.1249	.0664	2.9	2.9122	.2073	2.1	7.4617	.0125	4.3
.1742	.0850	3.2	3.0061	.2021	2.1	7.6151	.0118	4.4
.2246	.0942	3.3	3.1660	.1879	1.7	7.7734	.0130	4.3
.2750	.1119	3.2	3.3168	.1739	1.8	7.9366	.0135	4.0
.3265	.1215	3.2	3.4547	.1784	1.9	8.1050	.0138	3.9
.3743	.1322	2.7	3.6268	.1731	1.7	8.2789	.0153	3.7
.4260	.1246	2.6	3.7578	.1745	1.9	8.4585	.0146	3.6
.4737	.1367	2.6	3.8960	.1593	1.9	8.6441	.0152	3.6
.5263	.1419	2.5	4.0420	.1550	1.9	8.8358	.0151	3.5
.5757	.1468	2.5	4.1648	.1555	2.0	8.9341	.0122	4.4
.6233	.1440	2.6	4.2933	.1494	2.0	9.0340	.0136	4.5
.6769	.1424	2.5	4.4278	.1383	2.0	9.1357	.0120	4.5
.7261	.1525	2.5	4.5688	.1480	1.9	9.2390	.0104	4.8
.7745	.1692	2.4	4.7167	.1403	1.9	9.3442	.0107	4.9
.8279	.2012	2.1	4.8324	.1339	2.2	9.4511	.0096	4.9
.8870	.2064	2.0	4.9934	.1143	2.0	9.5599	.0088	5.1
.9527	.1952	1.9	5.1626	.1079	2.1	9.6707	.0090	5.2
1.0260	.1839	1.8	5.2504	.0993	2.7	9.7833	.0088	5.2
1.1080	.1863	1.7	5.3406	.1079	2.6	9.8980	.0076	5.3
1.2004	.2034	1.6	5.4331	.1016	2.6	10.0150	.0077	5.5
1.3048	.2005	1.5	5.5280	.1052	2.6	10.1330	.0078	5.4
1.3923	.1923	1.6	5.6254	.0953	2.6	10.2540	.0071	5.4
1.5060	.2017	1.4	5.7254	.0731	2.8	10.3780	.0059	5.8
1.5960	.2019	1.5	5.8282	.0309	3.8	10.5030	.0051	6.2
1.6943	.2035	1.4	5.9337	.0188	5.2	10.6310	.0050	6.4
1.8020	.2110	1.3	6.0422	.0187	5.3	10.7610	.0049	6.4
1.8957	.2112	1.4	6.1536	.0178	5.2	10.8930	.0041	6.7
1.9969	.2080	1.3	6.2682	.0149	5.4	11.0280	.0032	7.4
2.1065	.2140	1.3	6.3860	.0141	5.3	11.1650	.0019	8.7
2.1948	.2217	1.3	6.5072	.0159	4.9	11.3050	.0008	11.7
2.2887	.2187	1.3	6.6319	.0155	4.6	11.4480	.0003	17.8
2.3887	.2193	1.3	6.7603	.0164	4.4	11.5940	.0001	26.9
2.4591	.2147	1.4	6.8924	.0153	4.3	11.7420	.0000	38.7
2.5323	.2202	2.3	7.1685	.0162	4.0			

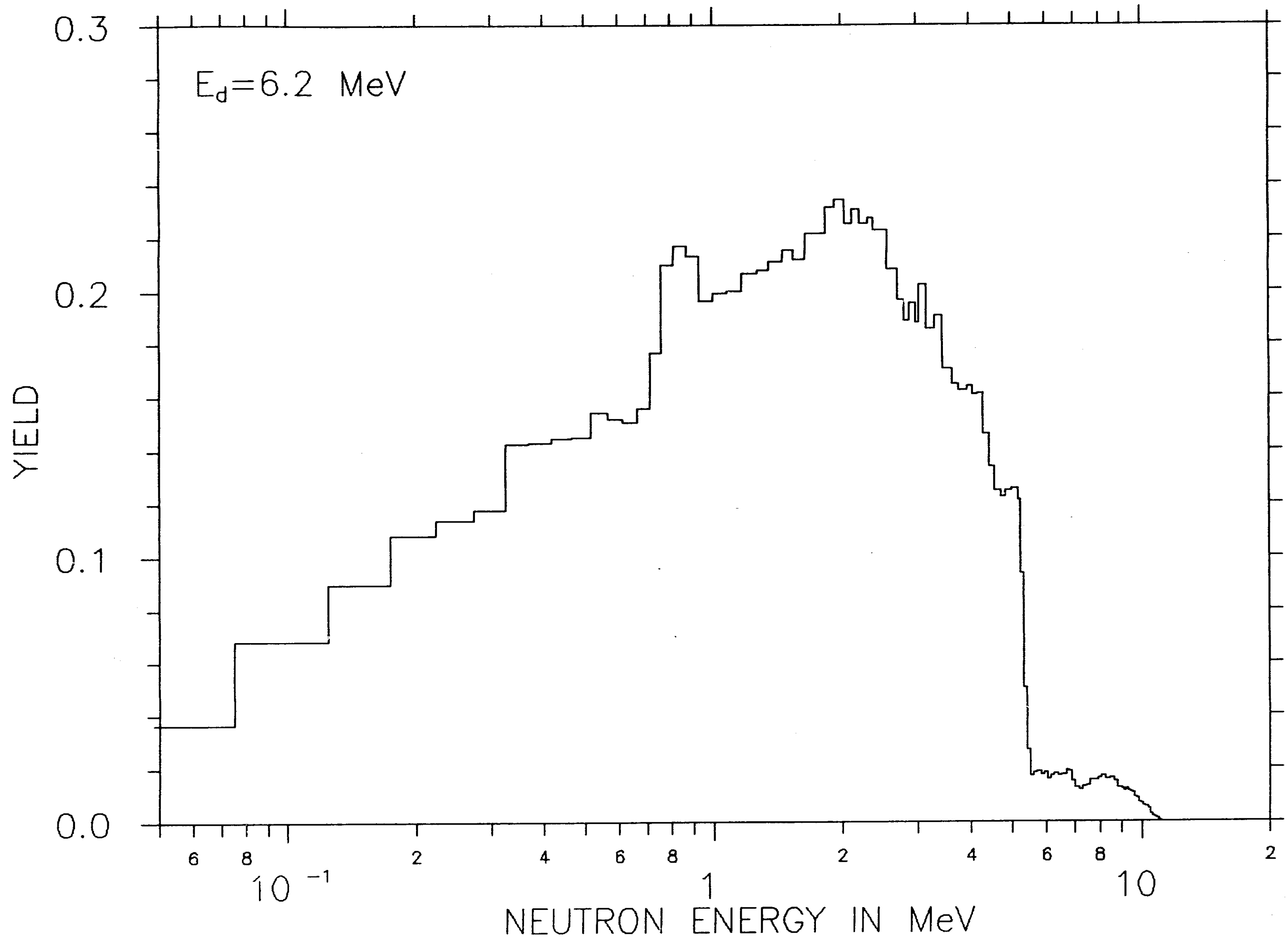

Fig. A-3. The normalized spectrum of neutrons emitted at 0 deg. with respect to 6.2 MeV deuterons incident on a thick Be-metal target.

Table A-IV. The normalized zero deg. neutron emission spectrum for 6.2-MeV deuterons on a thick Beryllium metal target.

Upper Edge MeV	Yield per MeV	Stat Err %	Upper Edge MeV	Yield per MeV	Stat Err %	Upper Edge MeV	Yield per MeV	Stat Err %
.0487	----	---	2.5562	.2231	1.7	6.7343	.0191	4.6
.0749	.0363	3.6	2.7139	.2079	1.5	6.8656	.0185	3.6
.1246	.0684	3.6	2.7983	.1967	2.0	7.0009	.0151	3.7
.1750	.0895	4.0	2.8867	.1890	2.0	7.1402	.0126	4.0
.2238	.1082	4.1	2.9793	.1956	1.9	7.2837	.0119	4.2
.2739	.1135	4.1	3.0371	.1880	2.4	7.4316	.0133	3.9
.3251	.1177	4.1	3.1577	.2027	1.7	7.5841	.0134	3.8
.3690	.1424	2.7	3.3079	.1857	1.6	7.7413	.0156	3.5
.4196	.1427	2.5	3.4452	.1910	1.6	7.9035	.0155	3.4
.4662	.1445	2.6	3.6166	.1703	1.5	8.0709	.0162	3.3
.5175	.1450	2.5	3.7470	.1648	1.8	8.2437	.0172	3.1
.5657	.1540	2.6	3.9131	.1626	1.6	8.4221	.0160	3.1
.6119	.1515	2.6	4.0300	.1642	1.8	8.6065	.0161	3.1
.6641	.1505	2.5	4.1522	.1609	1.8	8.7969	.0150	3.1
.7119	.1558	2.6	4.2801	.1611	1.7	8.8946	.0128	4.0
.7588	.1763	2.4	4.4141	.1461	1.8	8.9938	.0125	4.1
.8106	.2097	2.1	4.5544	.1339	1.8	9.0948	.0125	4.1
.8679	.2169	2.0	4.7016	.1248	1.8	9.1975	.0116	4.2
.9314	.2127	1.9	4.8167	.1225	2.0	9.3019	.0122	4.2
1.0022	.1963	1.8	4.9769	.1246	1.8	9.4081	.0113	4.1
1.0814	.1994	1.7	5.1453	.1256	1.7	9.5162	.0111	4.2
1.1703	.2001	1.6	5.2327	.1212	2.2	9.6261	.0107	4.2
1.2707	.2066	1.5	5.3224	.0936	2.4	9.7380	.0091	4.4
1.3548	.2076	1.6	5.4144	.0501	3.0	9.8519	.0088	4.6
1.4638	.2109	1.4	5.5088	.0267	4.2	9.9678	.0071	4.8
1.5500	.2151	1.5	5.6057	.0172	5.3	10.0860	.0067	5.2
1.6440	.2115	1.4	5.7052	.0184	5.3	10.2060	.0058	5.4
1.7469	.2219	1.3	5.8074	.0187	5.2	10.3280	.0053	5.6
1.8363	.2219	1.4	5.9124	.0176	5.0	10.4520	.0047	5.9
1.9327	.2311	1.3	6.0202	.0184	4.9	10.5790	.0029	6.7
2.0370	.2341	1.3	6.1311	.0159	4.9	10.7080	.0019	8.3
2.1209	.2255	1.4	6.2450	.0170	4.7	10.8400	.0014	9.7
2.2100	.2306	1.3	6.3622	.0177	4.4	10.9740	.0011	10.9
2.3049	.2252	1.3	6.4827	.0173	4.2	11.1100	.0005	13.5
2.3716	.2272	1.5	6.6700	.0174	3.4	11.2490	.0001	21.2

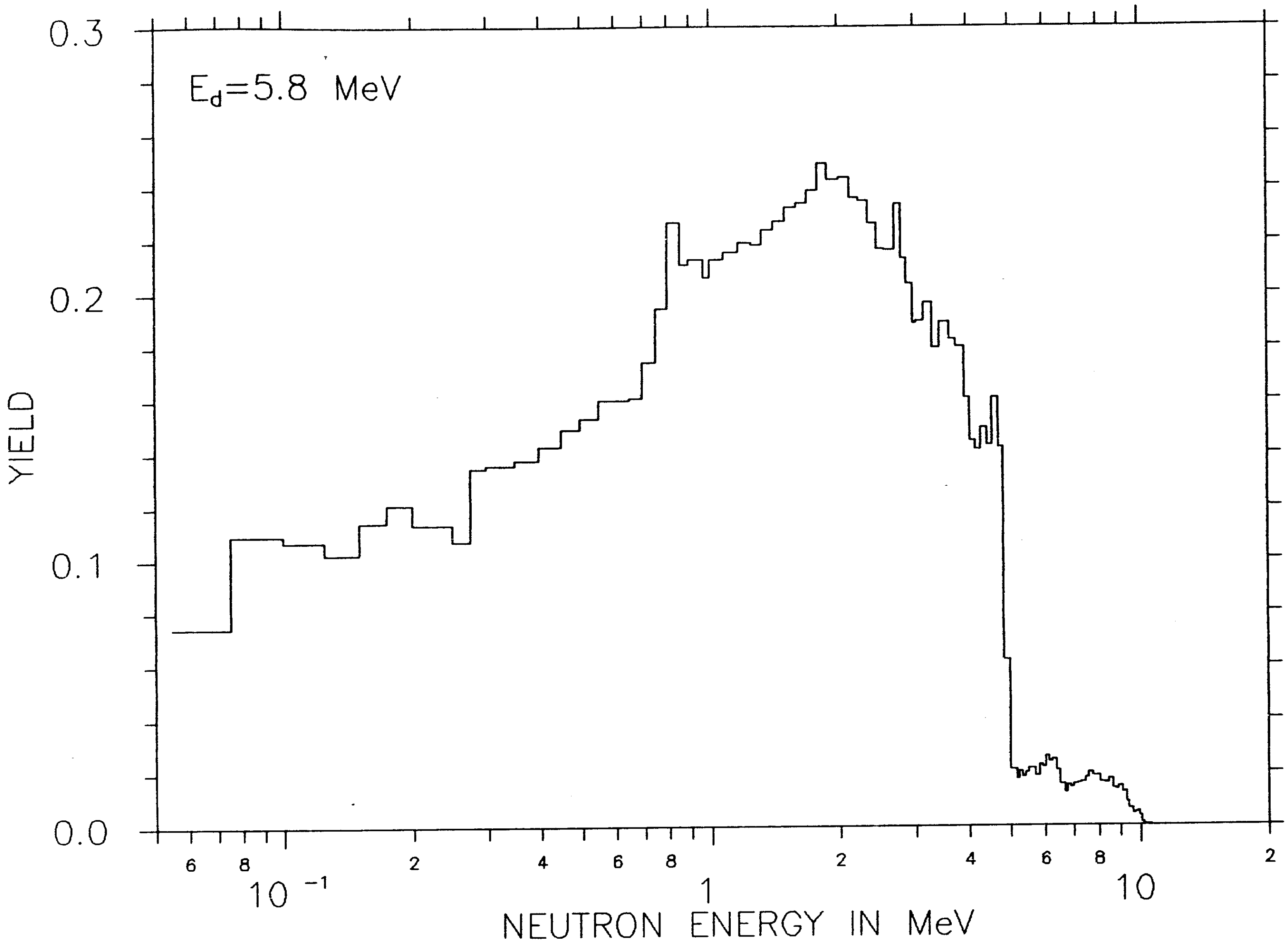

Fig. A-4. The normalized spectrum of neutrons emitted at 0 deg. with respect to 5.8 MeV deuterons incident on a thick Be-metal target.

Table A-V. The normalized zero deg. neutron emission spectrum for 5.8 MeV deuterons on a thick Beryllium metal target.

Upper Edge MeV	Yield per MeV	Stat Err %	Upper Edge MeV	Yield per MeV	Stat Err %	Upper Edge MeV	Yield per MeV	Stat Err %
.0548	----	---	2.4615	.2266	1.1	7.0009	.0145	4.5
.0749	.0743	5.5	2.5562	.2167	1.9	7.1402	.0153	4.4
.0999	.1090	4.9	2.7139	.2163	1.7	7.2837	.0160	4.2
.1249	.1067	5.1	2.7983	.2336	2.1	7.4316	.0162	4.0
.1504	.1018	5.4	2.8867	.2132	2.2	7.5841	.0181	3.8
.1749	.1140	5.4	2.9793	.2035	2.2	7.7413	.0199	3.6
.2003	.1207	5.2	3.0371	.1890	2.8	7.9035	.0187	3.5
.2489	.1133	4.0	3.1577	.1898	2.0	8.0709	.0186	3.5
.2740	.1069	5.7	3.3079	.1963	1.8	8.2437	.0163	3.6
.2996	.1344	5.3	3.4452	.1798	1.9	8.4221	.0159	3.7
.3497	.1357	3.8	3.6166	.1891	1.7	8.6065	.0173	3.5
.3972	.1376	3.9	3.7470	.1827	1.9	8.7969	.0140	3.6
.4489	.1427	3.7	3.9131	.1802	1.7	8.8946	.0135	4.6
.4963	.1494	3.8	4.0300	.1609	2.1	8.9938	.0148	4.5
.5517	.1531	3.4	4.1522	.1450	2.2	9.0948	.0149	4.4
.6485	.1602	2.7	4.2801	.1415	2.1	9.1975	.0124	4.5
.6966	.1610	2.3	4.4141	.1497	2.0	9.3019	.0127	4.7
.7480	.1743	2.1	4.5544	.1431	2.0	9.4081	.0089	5.0
.7978	.1943	2.0	4.7016	.1610	1.9	9.5162	.0064	5.9
.8527	.2270	1.8	4.8167	.1425	2.2	9.6261	.0064	6.3
.8955	.2107	2.0	4.9769	.0621	2.6	9.7380	.0044	6.9
.9710	.2127	1.6	5.1453	.0212	4.6	9.8519	.0048	7.4
1.0018	.2059	2.2	5.2327	.0177	6.8	9.9678	.0052	7.0
1.0796	.2128	1.5	5.3224	.0205	6.3	10.0860	.0036	7.4
1.1669	.2158	1.4	5.4144	.0183	6.4	10.2060	.0013	9.7
1.2503	.2193	1.4	5.5088	.0197	6.2	10.3280	.0004	15.8
1.3270	.2185	1.5	5.6057	.0216	5.8	10.4520	.0002	24.0
1.4109	.2241	1.4	5.7052	.0214	5.6	10.5790	.0002	27.2
1.5030	.2273	1.3	5.8074	.0188	5.7			
1.6044	.2327	1.2	5.9124	.0226	5.4			
1.6932	.2342	1.2	6.0202	.0219	5.2			
1.7896	.2388	1.2	6.1311	.0259	4.7			
1.8944	.2490	1.1	6.2450	.0240	4.4			
2.0087	.2428	1.1	6.3622	.0248	4.3			
2.1337	.2437	1.0	6.4827	.0206	4.3			
2.2353	.2362	1.1	6.6700	.0155	4.0			
2.3443	.2349	1.1	6.7343	.0124	6.2			
2.4615	.2266	1.1	6.8656	.0149	4.8			

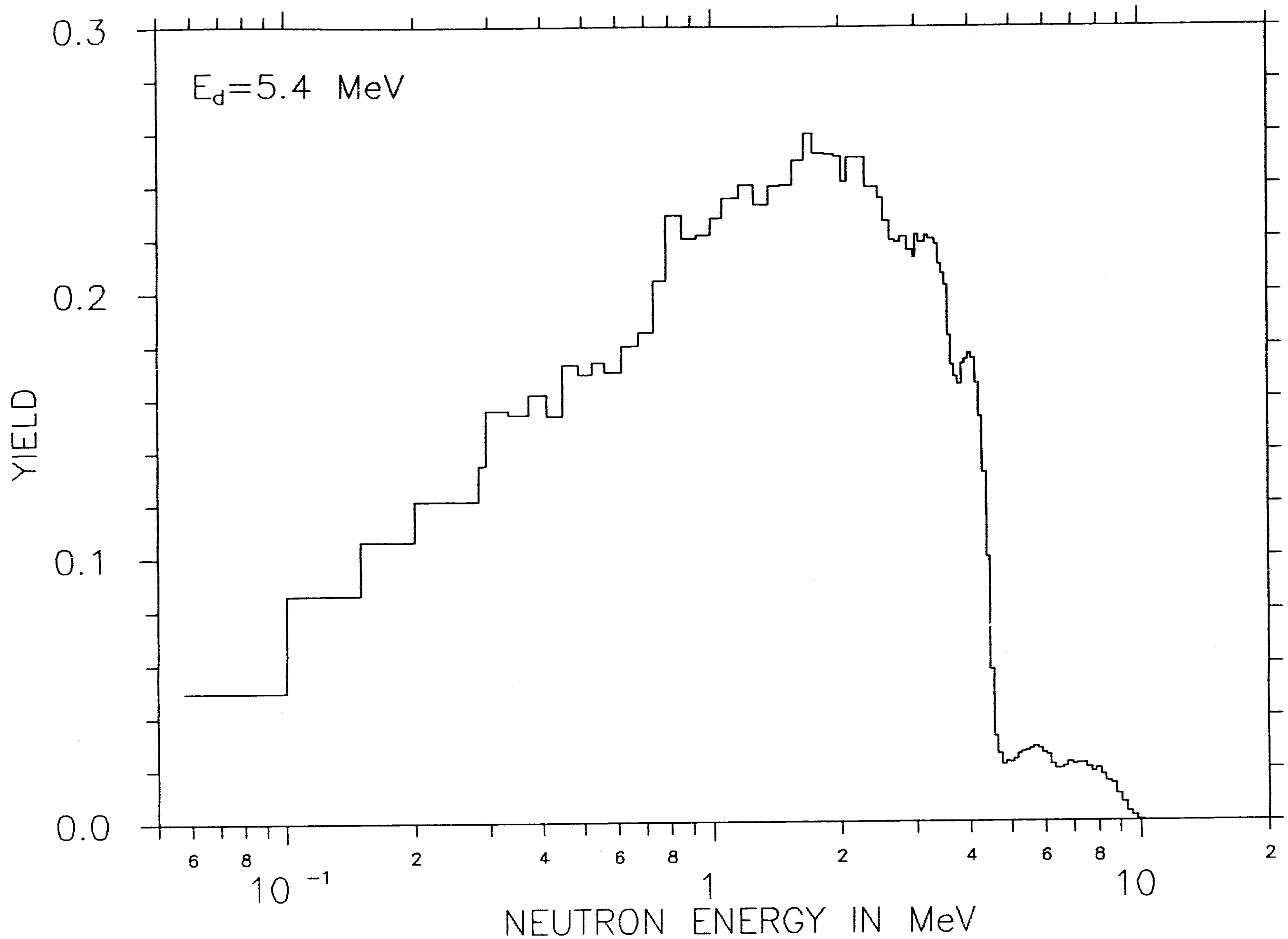

Fig. A-5. The normalized spectrum of neutrons emitted at 0 deg. with respect to 5.4 MeV deuterons incident on a thick Be-metal target.

Table A-VI. The normalized zero deg. neutron emission spectrum for 5.4 MeV deuterons on a thick Beryllium metal target.

Upper Edge MeV	Yield per MeV	Stat Err %	Upper Edge MeV	Yield per MeV	Stat Err %	Upper Edge MeV	Yield per MeV	Stat Err %
.0579	----	---	2.0786	.2415	2.0	4.5472	.0576	2.6
.1004	.0497	3.1	2.1954	.2504	1.5	4.6394	.0325	3.4
.1499	.0860	3.6	2.2896	.2505	1.7	4.7346	.0255	4.2
.2010	.1061	3.8	2.4607	.2392	1.3	4.8327	.0217	4.6
.2502	.1212	3.9	2.5345	.2354	1.8	4.9339	.0229	4.6
.2833	.1214	4.9	2.6117	.2266	1.8	5.0383	.0223	4.5
.2947	.1351	4.6	2.6926	.2195	1.8	5.1460	.0236	4.5
.3340	.1558	3.5	2.7772	.2185	1.8	5.2573	.0256	4.3
.3732	.1539	3.6	2.8659	.2206	1.7	5.3723	.0263	4.1
.4122	.1617	3.6	2.9589	.2156	1.7	5.4910	.0266	4.0
.4491	.1537	3.7	3.0071	.2130	2.1	5.6138	.0276	3.9
.4880	.1727	3.5	3.0565	.2213	2.1	5.7407	.0285	3.8
.5250	.1691	3.7	3.1072	.2185	2.0	5.8720	.0276	3.7
.5624	.1736	3.6	3.1591	.2186	2.0	6.0079	.0259	3.7
.6173	.1701	3.1	3.2123	.2209	2.0	6.1486	.0251	3.6
.6754	.1801	2.9	3.2669	.2198	2.0	6.2943	.0217	3.7
.7304	.1853	2.9	3.3229	.2197	1.9	6.4453	.0199	3.7
.7858	.2044	2.8	3.3803	.2176	1.9	6.6018	.0197	3.6
.8552	.2288	2.4	3.4393	.2103	1.9	6.7640	.0207	3.4
.9257	.2201	2.4	3.4998	.2070	1.9	6.9324	.0221	3.2
.9961	.2213	2.3	3.5619	.2023	1.9	7.1071	.0216	3.0
1.0644	.2277	2.3	3.6257	.1835	2.0	7.2886	.0220	2.9
1.1631	.2352	1.9	3.6913	.1723	2.0	7.4772	.0221	2.8
1.2628	.2402	1.8	3.7586	.1681	2.0	7.6732	.0202	2.8
1.3610	.2329	1.9	3.8278	.1653	2.0	7.8770	.0187	2.8
1.4546	.2400	1.9	3.8989	.1729	2.0	8.0892	.0199	2.7
1.5582	.2404	1.7	3.9721	.1743	1.9	8.3100	.0174	2.7
1.6532	.2494	1.8	4.0473	.1770	1.9	8.5401	.0153	2.8
1.7356	.2599	1.8	4.1247	.1750	1.9	8.7799	.0144	2.9
1.8477	.2521	1.6	4.2043	.1656	1.9	9.0301	.0102	3.1
1.9453	.2518	1.7	4.2863	.1529	1.9	9.2911	.0071	3.6
2.0237	.2509	1.8	4.3707	.1315	2.0	9.5637	.0035	4.5
2.0786	.2415	2.0	4.4576	.0995	2.2	9.8485	.0019	6.0

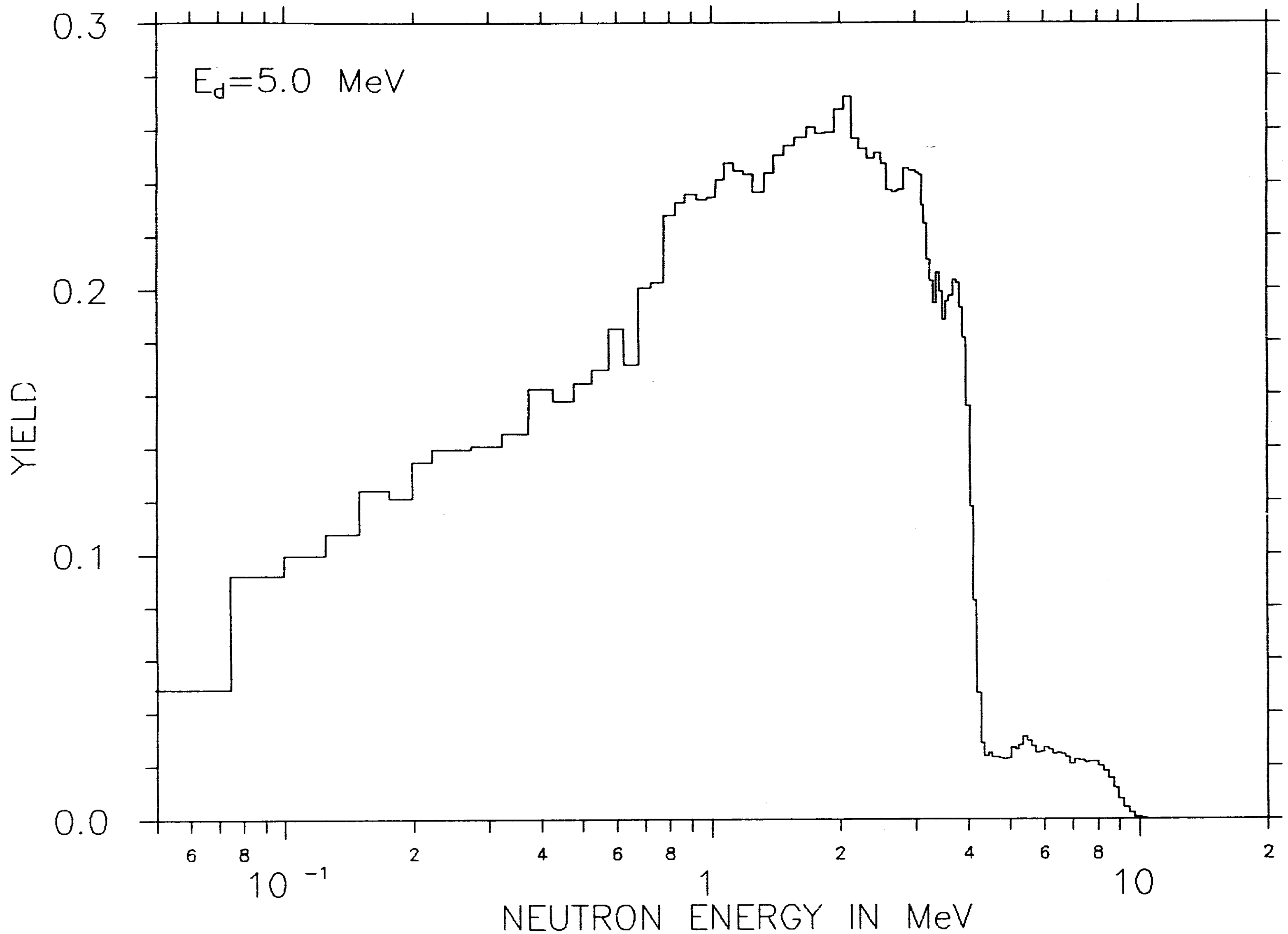

Fig. A-6. The normalized spectrum of neutrons emitted at 0 deg. with respect to 5.0 MeV deuterons incident on a thick Be-metal target.

Table A-VII. The normalized zero deg. neutron emission spectrum for 5.0-MeV deuterons on a thick Beryllium metal target.

Upper Edge MeV	Yield per MeV	Stat Err %	Upper Edge MeV	Yield per MeV	Stat Err %	Upper Edge MeV	Yield per MeV	Stat Err %
.0496	----	---	1.9428	.2589	1.6	4.5258	.0246	4.5
.0746	.0489	3.2	2.0479	.2674	1.5	4.6172	.0231	4.5
.1000	.0920	3.8	2.1324	.2722	1.6	4.7114	.0232	4.5
.1248	.0995	4.1	2.2223	.2567	1.6	4.8085	.0226	4.4
.1501	.1076	4.3	2.3180	.2527	1.6	4.9086	.0223	4.4
.1754	.1242	4.2	2.4200	.2491	1.5	5.0119	.0229	4.4
.1993	.1209	4.5	2.4918	.2510	1.7	5.1186	.0267	4.1
.2225	.1343	4.5	2.5669	.2469	1.7	5.2287	.0257	4.0
.2742	.1394	3.1	2.6454	.2371	1.7	5.3424	.0277	3.9
.3243	.1406	3.1	2.7276	.2364	1.7	5.4598	.0306	3.7
.3741	.1451	3.1	2.8137	.2372	1.6	5.5812	.0291	3.6
.4258	.1620	3.0	2.9039	.2454	1.6	5.7067	.0271	3.6
.4765	.1575	3.1	2.9985	.2445	1.5	5.8365	.0246	3.7
.5259	.1640	3.1	3.0476	.2437	1.9	5.9708	.0250	3.7
.5753	.1691	3.1	3.0979	.2430	1.8	6.1098	.0266	3.5
.6228	.1850	3.0	3.1494	.2313	1.8	6.2537	.0259	3.3
.6764	.1711	2.9	3.2023	.2246	1.9	6.4028	.0243	3.3
.7255	.2006	2.8	3.2564	.2108	1.9	6.5573	.0248	3.1
.7739	.2026	2.8	3.3120	.2030	1.9	6.7175	.0241	3.0
.8272	.2277	2.6	3.3690	.1944	1.9	6.8837	.0230	2.9
.8709	.2325	2.7	3.4275	.2063	1.9	7.0561	.0208	2.9
.9264	.2358	2.4	3.4876	.1988	1.9	7.2351	.0224	2.8
.9783	.2339	2.4	3.5492	.1881	1.9	7.4211	.0219	2.7
1.0250	.2345	2.5	3.6125	.1953	1.9	7.6144	.0212	2.7
1.0751	.2415	2.4	3.6775	.1974	1.8	7.8153	.0216	2.6
1.1290	.2475	2.3	3.7443	.2031	1.8	8.0244	.0216	2.5
1.1870	.2445	2.2	3.8129	.2020	1.8	8.2420	.0200	2.5
1.2497	.2432	2.1	3.8835	.1931	1.8	8.4686	.0180	2.5
1.3316	.2366	1.9	3.9560	.1812	1.8	8.7048	.0153	2.7
1.4062	.2438	1.9	4.0305	.1555	1.9	8.9510	.0114	2.9
1.4872	.2501	1.8	4.1072	.1175	2.1	9.2079	.0076	3.4
1.5755	.2539	1.7	4.1861	.0826	2.4	9.4761	.0045	4.1
1.6719	.2568	1.6	4.2674	.0472	2.9	9.7562	.0024	5.2
1.7555	.2611	1.7	4.3510	.0283	3.7	10.0490	.0008	7.2
1.8456	.2584	1.6	4.4371	.0236	4.4	10.3550	.0003	10.2

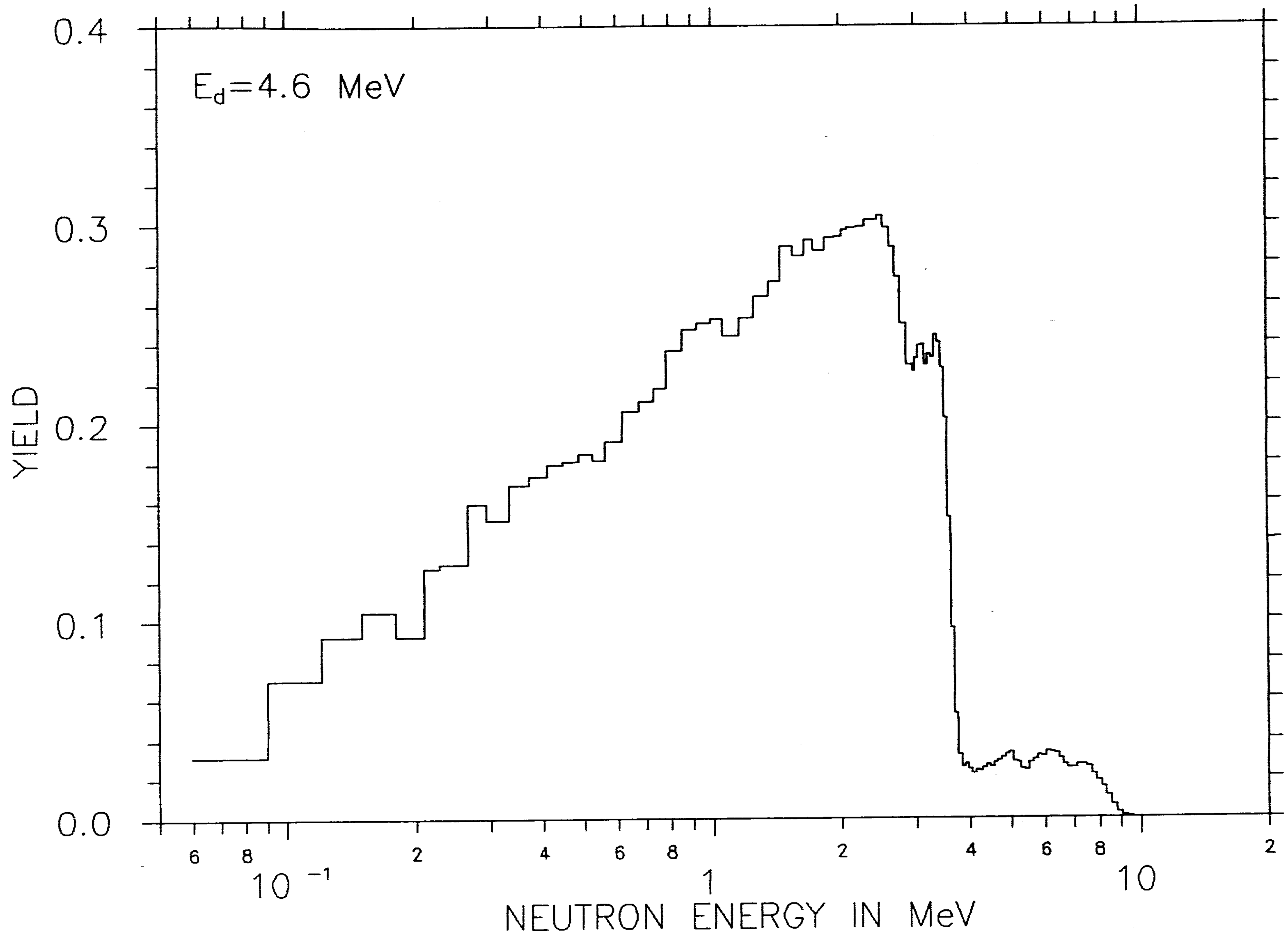

Fig. A–7. The normalized spectrum of neutrons emitted at 0 deg. with respect to 4.6 MeV deuterons incident on a thick Be–metal target.

Table A-VIII. The normalized zero deg. neutron emission spectrum for 4.6 MeV deuterons on a thick Beryllium metal target.

Upper Edge MeV	Yield per MeV	Stat Err %	Upper Edge MeV	Yield per MeV	Stat Err %	Upper Edge MeV	Yield per MeV	Stat Err %
.0599	----	---	1.9453	.2928	1.5	4.3707	.0248	4.6
.0899	.0315	3.0	2.0237	.2932	1.6	4.4576	.0263	4.4
.1205	.0702	4.3	2.0786	.2968	1.8	4.5472	.0256	4.3
.1497	.0923	4.9	2.1954	.2975	1.4	4.6394	.0275	4.2
.1793	.1044	5.1	2.2896	.2980	1.5	4.7346	.0288	4.1
.2093	.0921	5.6	2.4607	.3013	1.1	4.8327	.0301	3.9
.2282	.1266	6.5	2.5345	.3036	1.6	4.9339	.0318	3.8
.2669	.1286	4.7	2.6117	.2976	1.5	5.0383	.0331	3.7
.2947	.1587	4.1	2.6926	.2882	1.5	5.1460	.0280	3.7
.3340	.1506	3.4	2.7772	.2733	1.5	5.2573	.0276	3.9
.3732	.1687	3.3	2.8659	.2494	1.6	5.3723	.0246	3.9
.4122	.1729	3.3	2.9589	.2289	1.6	5.4910	.0242	4.0
.4491	.1789	3.3	3.0071	.2255	2.0	5.6138	.0276	3.8
.4880	.1805	3.3	3.0565	.2318	1.9	5.7407	.0292	3.6
.5250	.1840	3.4	3.1072	.2387	1.9	5.8720	.0311	3.4
.5624	.1806	3.4	3.1591	.2390	1.8	6.0079	.0310	3.3
.6173	.1902	2.8	3.2123	.2290	1.8	6.1486	.0334	3.1
.6754	.2059	2.6	3.2669	.2342	1.8	6.2943	.0330	3.0
.7304	.2110	2.6	3.3229	.2327	1.8	6.4453	.0322	2.8
.7858	.2169	2.6	3.3803	.2441	1.8	6.6018	.0298	2.8
.8552	.2362	2.2	3.4393	.2398	1.7	6.7640	.0267	2.8
.9257	.2470	2.1	3.4998	.2274	1.8	6.9324	.0248	2.8
.9961	.2502	2.1	3.5619	.2019	1.8	7.1071	.0249	2.7
1.0644	.2522	2.1	3.6257	.1515	2.0	7.2886	.0265	2.6
1.1631	.2436	1.8	3.6913	.0959	2.3	7.4772	.0264	2.5
1.2628	.2531	1.7	3.7586	.0526	3.0	7.6732	.0253	2.4
1.3610	.2637	1.7	3.8278	.0319	3.8	7.8770	.0218	2.5
1.4546	.2709	1.7	3.8989	.0256	4.5	8.0892	.0187	2.6
1.5582	.2887	1.5	3.9721	.0268	4.7	8.3100	.0156	2.7
1.6532	.2839	1.6	4.0473	.0245	4.7	8.5401	.0109	3.0
1.7356	.2921	1.6	4.1247	.0222	4.8	8.7799	.0065	3.6
1.8477	.2865	1.4	4.2043	.0240	4.8	9.0301	.0028	4.8
1.9453	.2928	1.5	4.2863	.0231	4.7	9.2911	.0008	7.1

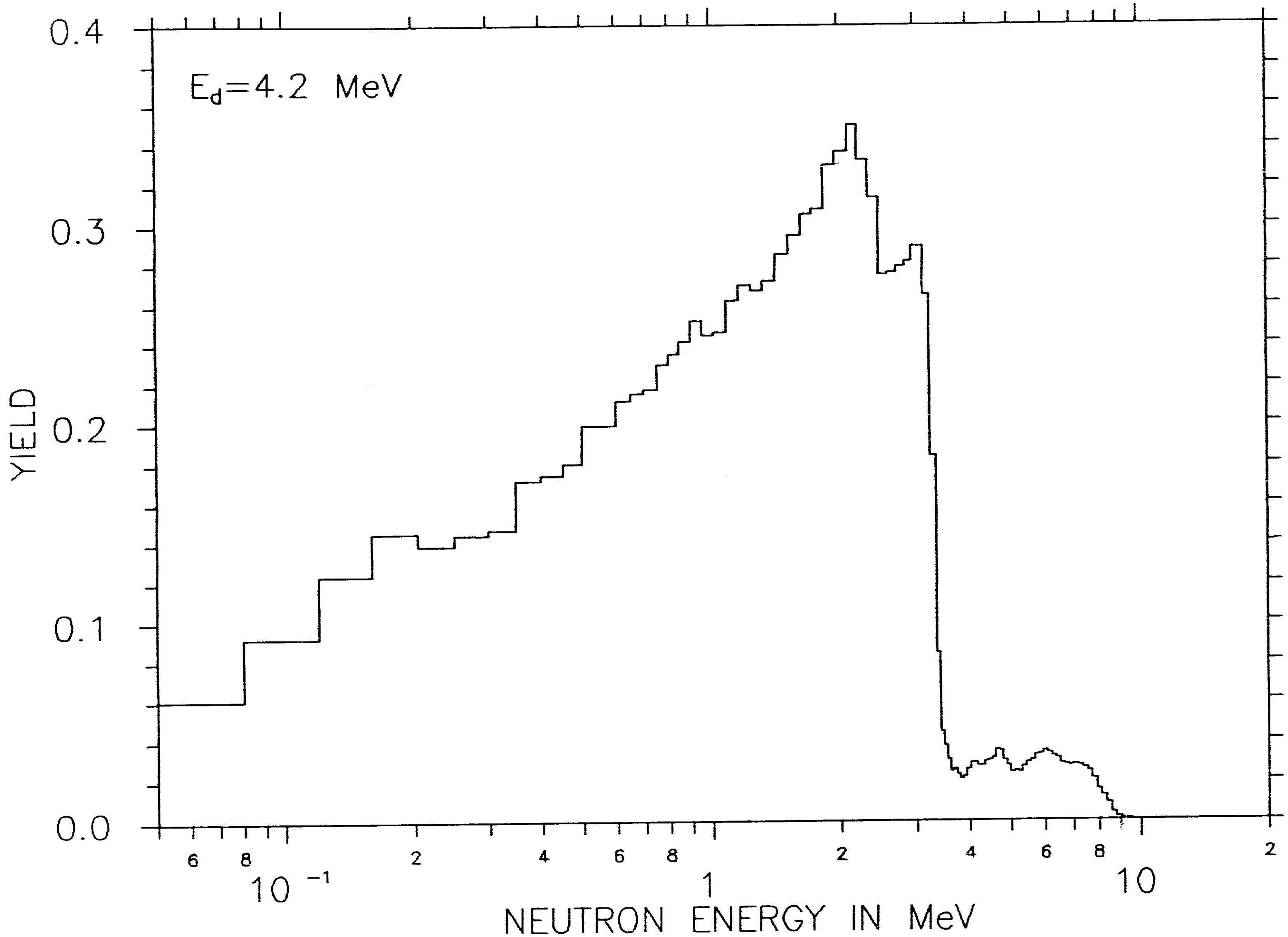

Fig. A–8. The normalized spectrum of neutrons emitted at 0 deg. with respect to 4.2 MeV deuterons incident on a thick Be–metal target.

Table A-IX. The normalized zero deg. neutron emission spectrum for 4.2-MeV deuterons on a thick Beryllium metal target.

Upper Edge MeV	Yield per MeV	Stat Err %	Upper Edge MeV	Yield per MeV	Stat Err %	Upper Edge MeV	Yield per MeV	Stat Err %
.0100	----	---	1.8479	.3079	1.4	4.6752	.0349	3.9
.0339	.0117	99.0	1.9698	.3300	1.3	4.7704	.0346	3.8
.0499	.0234	2.9	2.1042	.3365	1.2	4.8685	.0300	3.9
.0798	.0606	4.5	2.2219	.3502	1.3	4.9697	.0270	4.1
.1198	.0922	4.7	2.3497	.3323	1.3	5.0741	.0242	4.2
.1595	.1236	4.9	2.4889	.3138	1.2	5.1819	.0243	4.3
.2046	.1443	4.6	2.6017	.2747	1.4	5.2931	.0241	4.2
.2497	.1380	4.5	2.7222	.2760	1.4	5.4080	.0263	4.1
.3000	.1437	3.2	2.8514	.2790	1.3	5.5266	.0288	3.9
.3494	.1462	3.2	2.9427	.2816	1.5	5.6492	.0299	3.7
.4001	.1713	3.0	3.0384	.2894	1.5	5.7760	.0322	3.5
.4512	.1741	3.0	3.1389	.2890	1.4	5.9071	.0328	3.4
.4996	.1796	3.1	3.2445	.2646	1.4	6.0427	.0347	3.2
.6008	.1991	2.1	3.3556	.1833	1.6	6.1831	.0337	3.1
.6511	.2112	2.8	3.4132	.0840	2.5	6.3284	.0318	3.0
.6971	.2148	2.9	3.4724	.0440	3.4	6.4790	.0308	3.0
.7481	.2170	2.8	3.5331	.0374	4.2	6.6350	.0280	2.9
.7983	.2293	2.7	3.5955	.0304	4.6	6.7967	.0274	2.9
.8466	.2350	2.7	3.6595	.0246	5.0	6.9645	.0269	2.8
.8993	.2414	2.5	3.7252	.0256	5.1	7.1385	.0278	2.7
.9571	.2517	2.4	3.7928	.0230	5.2	7.3192	.0270	2.6
1.0206	.2446	2.2	3.8622	.0206	5.4	7.5069	.0261	2.5
1.0908	.2459	2.1	3.9335	.0220	5.4	7.7019	.0246	2.5
1.1684	.2619	2.0	4.0068	.0258	5.0	7.9047	.0209	2.6
1.2546	.2695	1.8	4.0822	.0288	4.7	8.1156	.0154	2.8
1.3363	.2666	1.9	4.1597	.0287	4.5	8.3352	.0123	3.1
1.4263	.2718	1.8	4.2395	.0270	4.5	8.5638	.0084	3.5
1.5257	.2853	1.6	4.3216	.0273	4.5	8.8020	.0039	4.4
1.6358	.2945	1.5	4.4061	.0291	4.4	9.0503	.0013	6.4
1.7370	.3052	1.5	4.4932	.0296	4.2	9.3094	.0003	9.9
1.8479	.3079	1.4	4.5828	.0307	4.1	9.5798	.0002	12.5

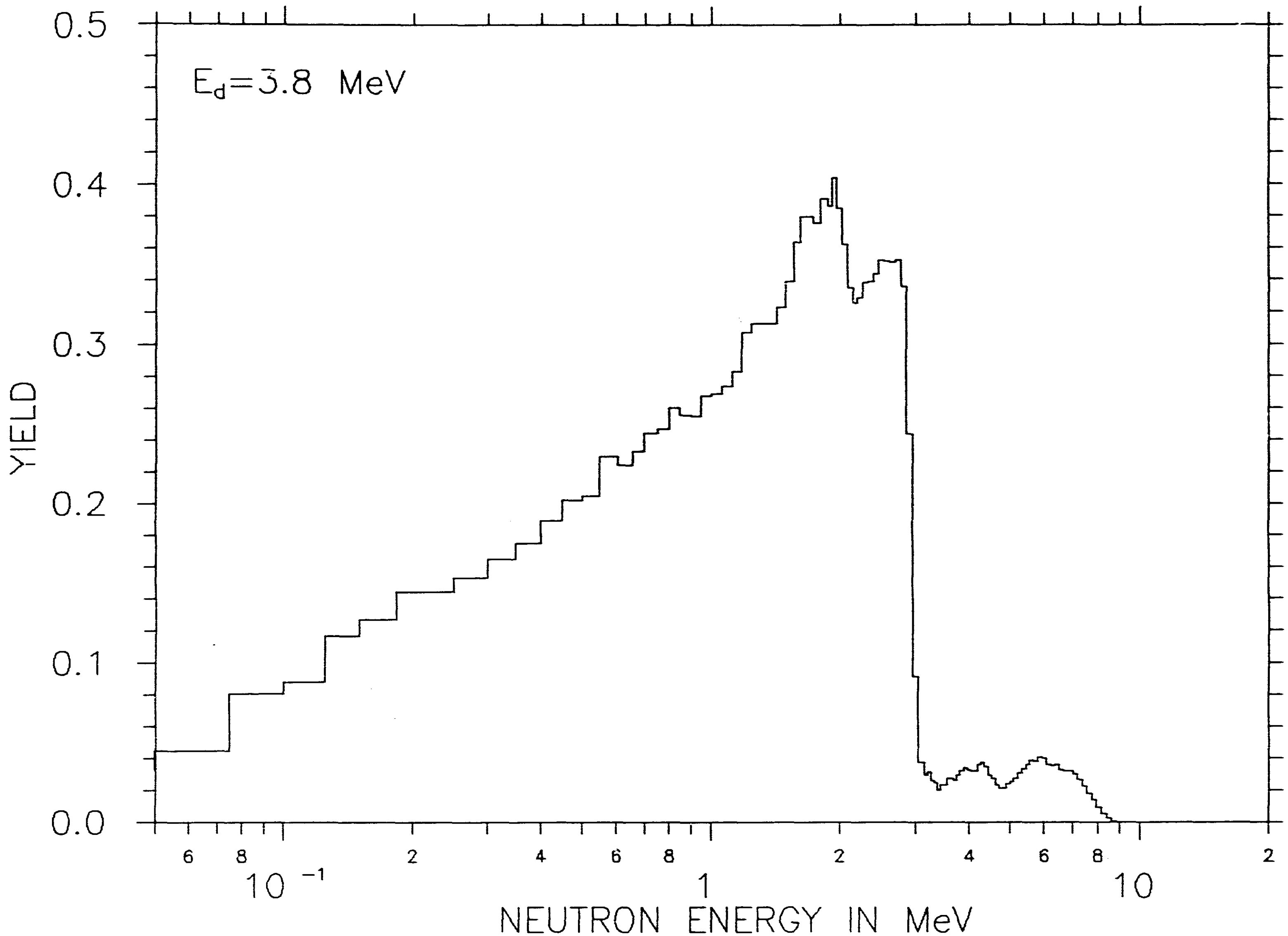

Fig. A-9. The normalized spectrum of neutrons emitted at 0 deg. with respect to 3.8 MeV deuterons incident on a thick Be-metal target.

Table A-X. The normalized zero deg. neutron emission spectrum for 3.8-MeV deuterons on a thick Beryllium metal target.

Upper Edge MeV	Yield per MeV	Stat Err %	Upper Edge MeV	Yield per MeV	Stat Err %	Upper Edge MeV	Yield per MeV	Stat Err %
.0372	----	---	1.7392	.3794	1.5	4.1676	.0318	3.2
.0498	.0328	6.5	1.8046	.3754	1.5	4.2476	.0359	3.7
.0748	.0447	6.1	1.8738	.3907	1.4	4.3300	.0370	3.6
.1001	.0808	6.7	1.9221	.3860	1.6	4.4147	.0346	3.6
.1248	.0881	7.0	1.9724	.4043	1.5	4.5020	.0293	3.8
.1498	.1163	6.7	2.0246	.3851	1.5	4.5919	.0273	3.9
.1832	.1266	5.8	2.0790	.3621	1.5	4.6846	.0230	4.1
.2498	.1437	4.3	2.1356	.3346	1.6	4.7801	.0213	4.3
.3002	.1527	2.9	2.1946	.3253	1.6	4.8785	.0212	4.3
.3496	.1647	2.9	2.2560	.3286	1.5	4.9800	.0237	4.2
.4003	.1744	2.8	2.3200	.3384	1.5	5.0848	.0250	4.0
.4487	.1889	2.8	2.3868	.3389	1.5	5.1929	.0272	3.8
.4999	.2017	2.6	2.4566	.3436	1.4	5.3044	.0307	3.6
.5490	.2045	2.7	2.5294	.3523	1.4	5.4197	.0334	3.4
.6013	.2292	2.5	2.6055	.3516	1.3	5.5387	.0357	3.2
.6516	.2242	2.5	2.6852	.3508	1.3	5.6617	.0383	3.0
.6976	.2329	2.6	2.7685	.3521	1.3	5.7889	.0377	3.0
.7487	.2438	2.4	2.8558	.3355	1.3	5.9205	.0405	2.9
.7990	.2466	2.4	2.9473	.2432	1.4	6.0565	.0398	2.7
.8473	.2600	2.4	3.0433	.0915	2.0	6.1974	.0361	2.7
.9001	.2551	2.3	3.1441	.0375	3.3	6.3433	.0354	2.7
.9493	.2546	2.3	3.1964	.0291	4.7	6.4943	.0357	2.6
1.0028	.2674	2.1	3.2500	.0312	4.7	6.6509	.0323	2.5
1.0609	.2688	2.0	3.3049	.0258	4.8	6.8132	.0317	2.5
1.1241	.2733	1.9	3.3613	.0243	5.1	6.9816	.0322	2.4
1.1813	.2827	2.0	3.4191	.0199	5.3	7.1563	.0299	2.3
1.2430	.3073	1.8	3.4784	.0229	5.3	7.3377	.0264	2.3
1.3096	.3131	1.7	3.5393	.0230	5.1	7.5261	.0223	2.4
1.3668	.3125	1.8	3.6018	.0274	4.9	7.7219	.0176	2.6
1.4278	.3131	1.8	3.6660	.0272	4.6	7.9254	.0138	2.8
1.4931	.3227	1.7	3.7319	.0262	4.6	8.1372	.0094	3.2
1.5629	.3386	1.6	3.7996	.0291	4.5	8.3576	.0053	3.9
1.6186	.3633	1.7	3.8692	.0317	4.2	8.5872	.0022	5.2
1.6772	.3796	1.6	3.9407	.0338	4.0	8.8264	.0006	7.8
1.7392	.3794	1.5	4.0142	.0324	4.0	9.0757	.0001	11.6

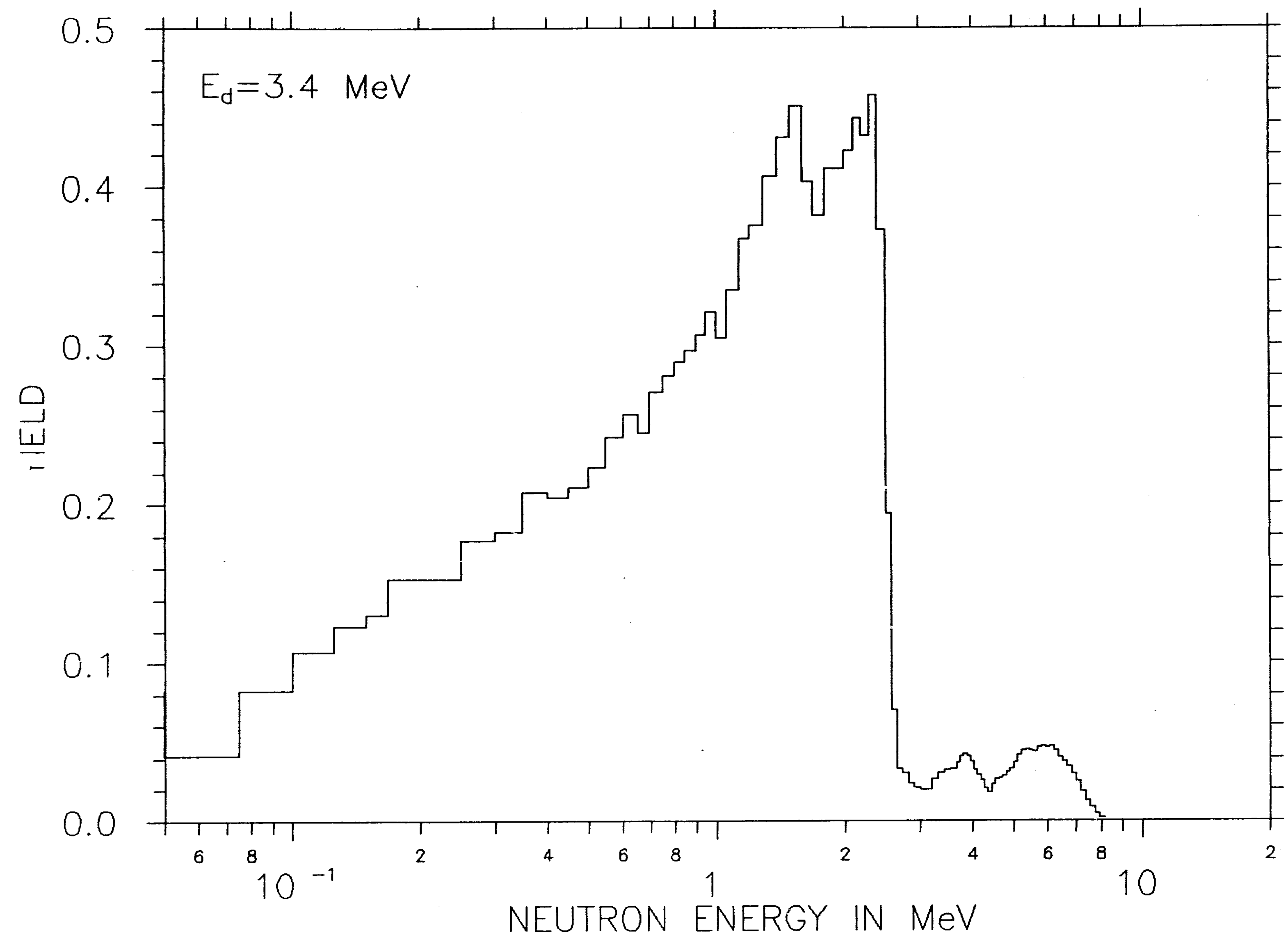

Fig. A−10. The normalized spectrum of neutrons emitted at 0 deg. with respect to 3.4 MeV deuterons incident on a thick Be−metal target.

Table A-XI. The normalized zero deg. neutron emission spectrum for 3.4-MeV deuterons on a thick Beryllium metal target.

Upper Edge MeV	Yield per MeV	Stat Err %	Upper Edge MeV	Yield per MeV	Stat Err %	Upper Edge MeV	Yield per MeV	Stat Err %
.0354	----	---	1.4931	.4317	1.7	4.3300	.0206	6.3
.0497	.0827	.0	1.5997	.4512	1.6	4.4147	.0180	6.8
.0748	.0416	6.0	1.6975	.4033	1.7	4.5020	.0229	6.5
.0996	.0823	7.4	1.8046	.3822	1.7	4.5919	.0264	5.9
.1251	.1063	7.7	1.9983	.4115	1.3	4.6846	.0269	5.6
.0149	.1233	8.0	2.1070	.4227	1.6	4.7801	.0283	5.4
.1681	.1306	9.2	2.1946	.4434	1.7	4.8785	.0310	5.2
.2498	.1525	5.6	2.2877	.4328	1.6	4.9800	.0330	5.0
.3002	.1771	3.8	2.3868	.4578	1.5	5.0848	.0369	4.7
.3496	.1827	3.8	2.4926	.3726	1.6	5.1929	.0417	4.4
.4003	.2074	3.6	2.5670	.1943	2.3	5.3044	.0445	4.1
.4487	.2040	3.7	2.6449	.0702	3.5	5.4197	.0453	4.0
.4999	.2108	3.6	2.7264	.0335	5.3	5.5387	.0447	3.9
.5490	.2235	3.6	2.8117	.0308	5.8	5.6617	.0442	3.9
.6013	.2418	3.4	2.9010	.0236	6.3	5.7889	.0463	3.8
.6516	.2568	3.3	2.9948	.0214	6.6	5.9205	.0470	3.7
.6976	.2450	3.5	3.1964	.0196	5.2	6.0565	.0464	3.6
.7487	.2705	3.2	3.3049	.0265	5.8	6.1974	.0469	3.4
.7990	.2808	3.2	3.4191	.0306	5.3	6.3433	.0447	3.3
.8473	.2891	3.2	3.5393	.0326	5.0	6.4943	.0404	3.3
.9001	.2966	3.0	3.6660	.0328	4.9	6.6509	.0379	3.3
.9493	.3068	3.0	3.7319	.0370	5.6	6.8132	.0345	3.2
1.0028	.3216	2.7	3.7996	.0414	5.3	6.9816	.0297	3.3
1.0609	.3047	2.7	3.8692	.0424	5.1	7.1563	.0255	3.4
1.1352	.3356	2.3	3.9407	.0411	5.0	7.3377	.0188	3.7
1.2054	.3672	2.2	4.0142	.0381	5.1	7.5261	.0126	4.2
1.2958	.3752	2.0	4.0898	.0323	5.3	7.7219	.0084	5.0
1.3968	.4068	1.8	4.1676	.0291	5.6	7.9254	.0043	6.1
1.4931	.4317	1.7	4.2476	.0260	5.9	8.1372	.0018	8.4

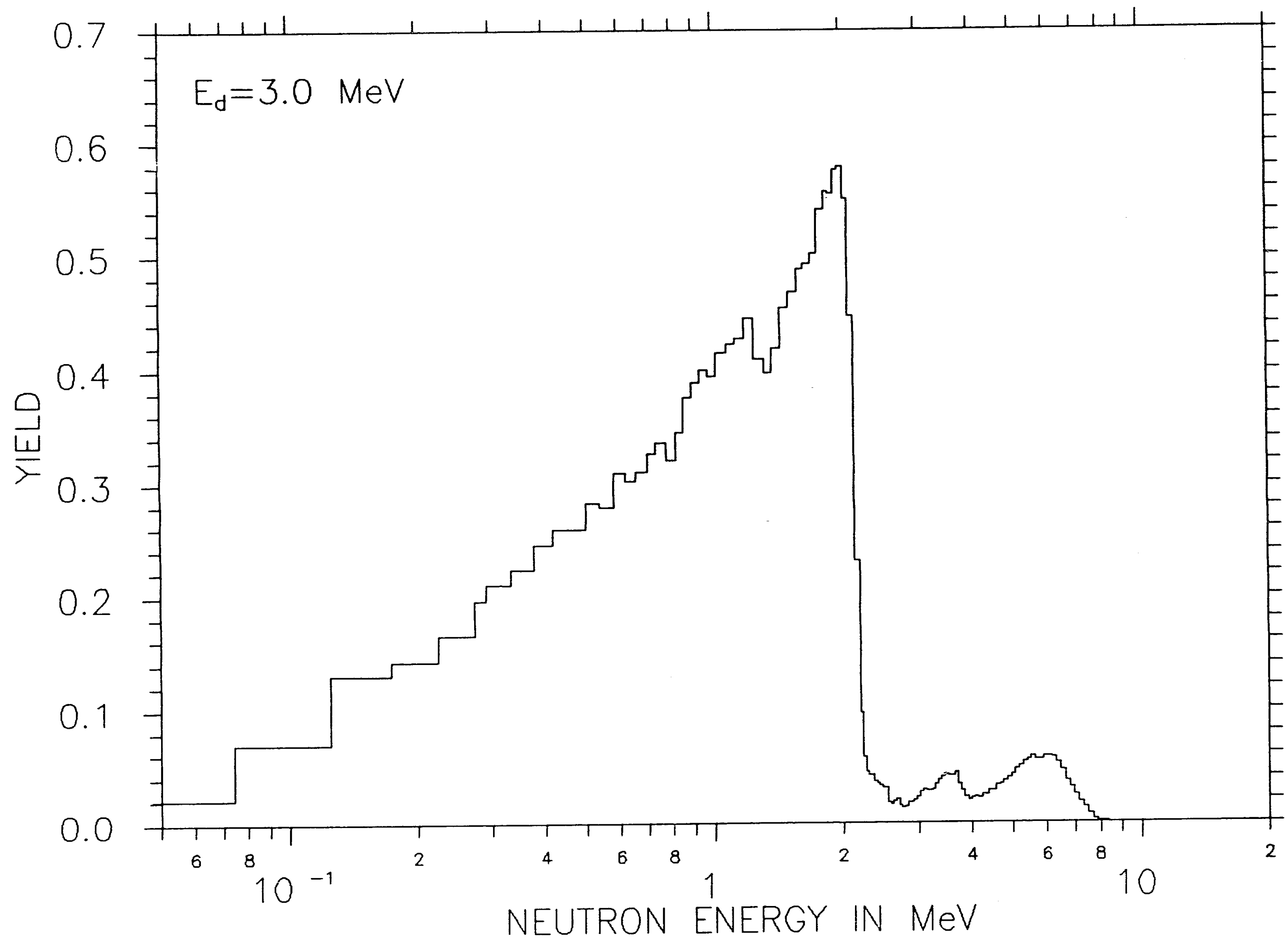

Fig. A-11. The normalized spectrum of neutrons emitted at 0 deg. with respect to 3.0 MeV deuterons incident on a thick Be-metal target.

Table A-XII. The normalized zero deg. neutron emission spectrum for 3.0-MeV deuterons on a thick Beryllium metal target.

Upper Edge MeV	Yield per MeV	Stat Err %	Upper Edge MeV	Yield per MeV	Stat Err %	Upper Edge MeV	Yield per MeV	Stat Err %
.0474	----	---	1.8788	.5575	1.5	3.7040	.0433	4.2
.0743	.0210	3.8	1.9277	.5554	1.5	3.7715	.0333	4.4
.1249	.0694	4.3	1.9786	.5771	1.5	3.8409	.0274	4.8
.1742	.1302	4.3	2.0316	.5800	1.4	3.9122	.0221	5.2
.2246	.1424	4.3	2.0867	.5505	1.4	3.9855	.0194	5.6
.2750	.1650	4.2	2.1441	.4470	1.5	4.0610	.0217	5.6
.2916	.1958	3.2	2.2039	.2302	1.9	4.1385	.0225	5.3
.3338	.2103	3.1	2.2347	.0968	3.3	4.2184	.0214	5.3
.3771	.2227	3.0	2.2662	.0581	4.3	4.3005	.0236	5.1
.4191	.2454	3.0	2.2984	.0444	5.2	4.3851	.0237	5.0
.4598	.2597	3.0	2.3312	.0423	5.6	4.4722	.0277	4.7
.4999	.2597	3.0	2.3648	.0423	5.6	4.5620	.0275	4.5
.5382	.2826	3.0	2.3991	.0365	5.7	4.6545	.0327	4.3
.5811	.2792	2.8	2.4341	.0344	5.9	4.7498	.0334	4.0
.6201	.3104	2.8	2.4700	.0324	6.1	4.8482	.0364	3.9
.6581	.3028	2.8	2.5066	.0307	6.2	4.9496	.0394	3.7
.6998	.3112	2.7	2.5440	.0308	6.2	5.0542	.0416	3.5
.7336	.3264	2.9	2.5823	.0175	6.8	5.1622	.0464	3.4
.7764	.3357	2.5	2.6215	.0154	8.0	5.2737	.0494	3.2
.8161	.3212	2.7	2.6616	.0189	7.8	5.3889	.0531	3.0
.8515	.3457	2.7	2.7025	.0204	7.2	5.5079	.0544	2.9
.8893	.3762	2.5	2.7445	.0152	7.5	5.6309	.0574	2.8
.9297	.3890	2.4	2.7874	.0128	8.2	5.7581	.0552	2.8
.9729	.4002	2.2	2.8314	.0141	8.3	5.8897	.0552	2.8
1.0192	.3947	2.1	2.8764	.0173	7.7	6.0258	.0581	2.6
1.0793	.4152	1.9	2.9225	.0175	7.3	6.1667	.0580	2.5
1.1335	.4232	1.9	2.9697	.0190	7.1	6.3127	.0571	2.4
1.1919	.4277	1.8	3.0180	.0219	6.7	6.4639	.0521	2.4
1.2549	.4451	1.7	3.0676	.0266	6.1	6.6207	.0457	2.4
1.3230	.4097	1.7	3.1183	.0289	5.7	6.7832	.0361	2.5
1.3816	.3976	1.8	3.1704	.0283	5.6	6.9519	.0303	2.6
1.4442	.4191	1.7	3.2238	.0282	5.5	7.1269	.0240	2.8
1.5112	.4547	1.6	3.2785	.0289	5.5	7.3087	.0179	3.1
1.5829	.4684	1.5	3.3347	.0333	5.2	7.4975	.0128	3.4
1.6401	.4884	1.6	3.3923	.0372	4.8	7.6938	.0069	4.1
1.7005	.4931	1.5	3.4514	.0404	4.6	7.8980	.0029	5.6
1.7642	.5021	1.5	3.5121	.0423	4.4	8.1104	.0010	8.0
1.8317	.5418	1.4	3.5743	.0407	4.3	8.3315	.0004	10.9
1.8788	.5575	1.5	3.6383	.0412	4.3	8.5619	.0001	12.5

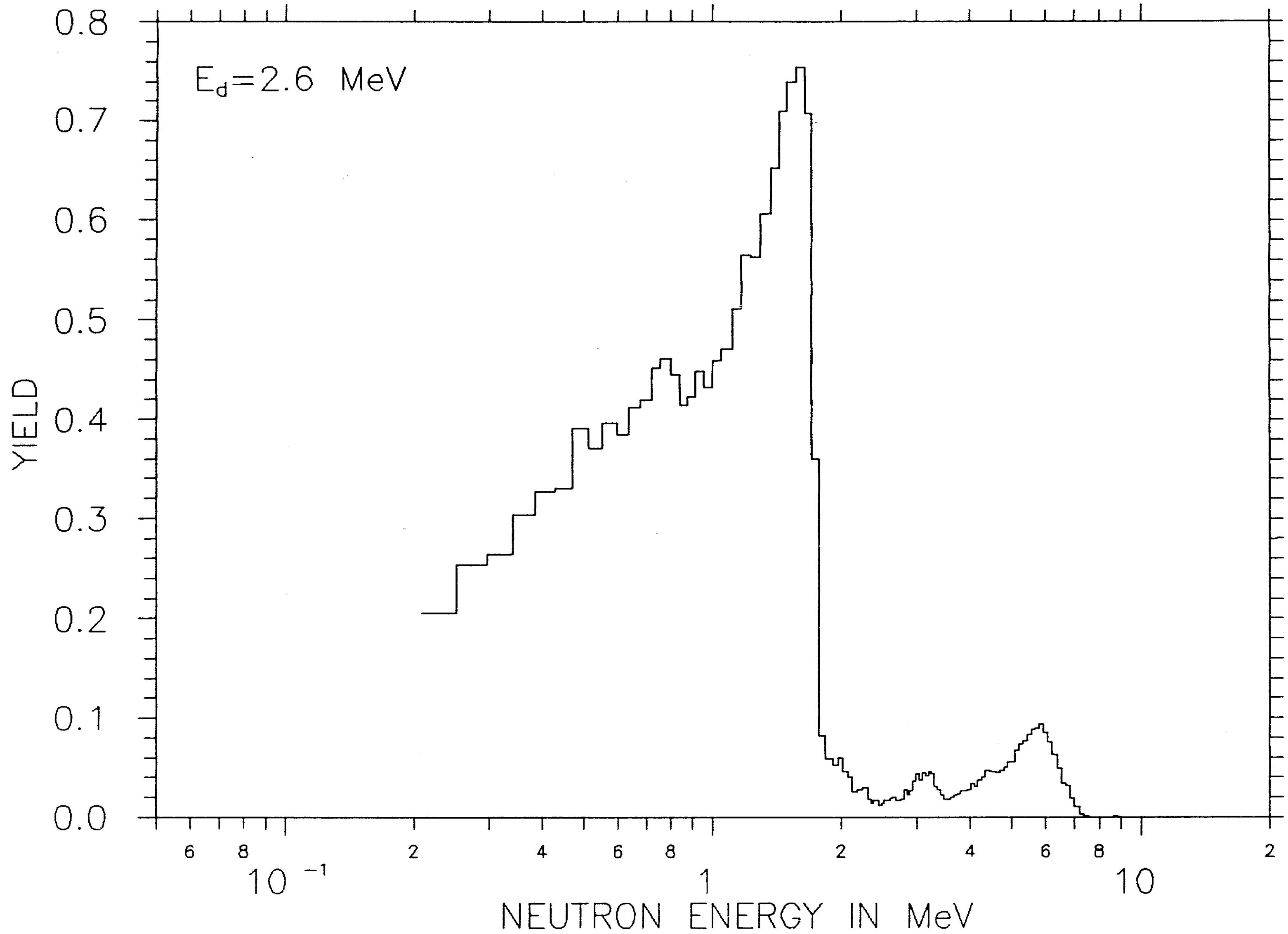

Fig. A−12. The normalized spectrum of neutrons emitted at 0 deg. with respect to 2.6 MeV deuterons incident on a thick Be−metal target.

Table A-XIII. The normalized zero deg. neutron emission spectrum for 2.6 MeV deuterons on a thick Beryllium metal target.

Upper Edge MeV	Yield per MeV	Stat Err %	Upper Edge MeV	Yield per MeV	Stat Err %	Upper Edge MeV	Yield per MeV	Stat Err %
.2085	----	---	2.0128	.0599	5.8	3.7921	.0231	7.4
.2525	.2054	4.0	2.0672	.0461	6.1	3.8621	.0268	6.9
.2965	.2535	3.7	2.1237	.0398	6.5	3.9340	.0267	6.6
.3398	.2646	3.7	2.1827	.0254	7.7	4.0079	.0277	6.5
.3843	.3036	3.4	2.2441	.0270	7.7	4.0840	.0336	6.1
.4276	.3278	3.4	2.3082	.0292	7.3	4.1622	.0311	5.9
.4695	.3308	3.4	2.3412	.0177	10.0	4.2428	.0366	5.7
.5110	.3919	3.2	2.3750	.0140	11.4	4.3256	.0403	5.3
.5506	.3715	3.4	2.4095	.0170	11.4	4.4110	.0468	4.9
.5949	.3966	3.1	2.4448	.0166	10.9	4.4989	.0460	4.7
.6353	.3851	3.2	2.4809	.0118	11.7	4.5895	.0461	4.6
.6748	.4132	3.1	2.5177	.0138	12.1	4.6828	.0447	4.6
.7181	.4202	3.0	2.5554	.0174	11.0	4.7790	.0465	4.6
.7533	.4524	3.2	2.5940	.0166	10.5	4.8782	.0500	4.4
.7979	.4619	2.8	2.6334	.0191	10.2	4.9806	.0551	4.2
.8392	.4463	2.9	2.6737	.0204	9.6	5.0862	.0554	4.0
.8762	.4151	3.1	2.7150	.0164	9.9	5.1953	.0665	3.8
.9157	.4237	3.0	2.7573	.0172	10.2	5.3079	.0733	3.5
.9579	.4489	2.8	2.8005	.0177	9.9	5.4242	.0766	3.3
1.0031	.4335	2.7	2.8448	.0271	8.8	5.5444	.0830	3.2
1.0516	.4603	2.6	2.8901	.0225	8.3	5.6686	.0878	3.0
1.1146	.4720	2.2	2.9365	.0267	8.3	5.7971	.0892	2.9
1.1715	.5127	2.2	2.9840	.0364	7.3	5.9300	.0941	2.8
1.2329	.5657	2.0	3.0327	.0436	6.4	6.0676	.0852	2.8
1.2993	.5637	2.0	3.0827	.0366	6.4	6.2100	.0752	2.8
1.3711	.6064	1.8	3.1338	.0441	6.3	6.3575	.0626	2.9
1.4330	.6524	1.8	3.1863	.0419	6.0	6.5104	.0490	3.1
1.4991	.7096	1.7	3.2400	.0455	5.9	6.6688	.0343	3.4
1.5700	.7399	1.6	3.2952	.0439	5.8	6.8332	.0317	3.6
1.6460	.7547	1.5	3.3518	.0305	6.3	7.0037	.0192	4.0
1.7067	.7076	1.7	3.4098	.0275	7.0	7.1807	.0101	5.0
1.7708	.3605	2.1	3.4694	.0222	7.5	7.3646	.0029	7.1
1.8386	.0815	3.9	3.5306	.0177	8.2	7.5556	.0006	12.1
1.9104	.0583	5.2	3.5934	.0182	8.5	7.7542	.0001	17.9
1.9606	.0520	6.2	3.6578	.0197	8.2	7.9608	.0000	15.7
2.0128	.0599	5.8	3.7241	.0218	7.8	8.1758	.0001	15.6

END

DATE
FILMED
3 / 16 / 92